Tampere University

Hamza Javedan

A Low-Cost Fatigue Tester for Maker Spaces

Faculty of Engineering and Natural Sciences
Master's Thesis
Prof. Roel Pieters
Metodi Netzev
September 2021

ABSTRACT

Hamza Javedan: A Low-Cost Fatigue Tester for Maker Spaces
Master's Thesis
Tampere University
Automation Engineering
September 2021

The fatigue testing machines (FTMs) commonly available in the market can cost upwards of a hundred thousand euros and require a pneumatic or hydraulic power supply. The pricetag and infrastructural needs of such devices make them unfeasible for maker space applications. A low-cost FTM designed for modularity and flexibility and constructed using easily accessible components can provide a viable alternative. The problem statement is addressed by identifying motors as the right actuation choice and selecting the motor type to accomplish the required operation based on the selection chart developed in this thesis. A hybrid bipolar stepper motor is selected for its precision, speed and torque characteristics. An h-bridge driver circuit is discussed for controlling motor rotation for high current applications. AutoDesk's TinkerCad model illustrates the motor control circuitry and the microcontroller programming necessary to control the motor. The control system is simulated on MATLAB/Simulink. Using a step input controlled PWM, position and speed control, and an h-bridge driver circuit to manage rotation, the motor is driven at different speeds for a variety of test scenarios. The motor has a step angle of 1.8 degrees. The shaft angle graphs demonstrate a cycle frequency of 0.5 Hz for unidirectional and bidirectional motor control. The required 70 Nm torque range, 0.5mm stroke size, and motor speed are dependent on the mechanical coupling used with the actuation system. The results validate the system's adaptability and flexibility for varying fatigue tests and require further research and practical experiments to develop a feasible standardized low-cost alternative for the growing maker space ecosystem.

Keywords: 3D printing, fatigue testing machines, h-bridge, hybrid bipolar stepper motor, maker space, PWM

PREFACE

This thesis work was carried out in the Department of Factory Automation and Robotics, Automation Engineering, at Tampere University, Tampere, Finland.

This thesis is the fruit of labor of an entire army of friends continually supporting me throughout this arduous adventure, without whom I could have never brought this research to completion. I want to express my deepest and sincerest gratitude to Professor Roel Pieters and Mr. Metodi Netzev for their patience, kindness, understanding, and counseling throughout this process. My warmest thanks to Aditya Premi, who went above and beyond the call of duty, for sharing in my frustrations, and encouraging me to get this thesis over the finish line. I want to acknowledge, in alphabetical order, Ahmed Kamal, Aoun Muhammad, Jayesh Gupta, Jazib Javed, Mohsin Shakoor, Uzair Ahmed, Ramyakrishna Jayanthi, and Shruti Mittal for being constant sources of motivation, and for their unwavering moral and emotional support, throughout this journey. I am in a debt of gratitude to these lovely humans.

Finally, I would like to thank my entire family for their patience and support during this entire saga that is my master's study. I wish to end this section with a quote by Mawlana Jalaluddin Muhammad Rumi, the 13th century Persian Sufi mystic and poet, which I find beautiful even though I don't understand it.

"What you seek is seeking you" - Rumi

Tampere, September 15, 2021

Hamza Javedan

CONTENTS

LIST OF FIGURES

LIST OF SYMBOLS AND ABBREVIATIONS

FTM	Fatigue Testing Machine
HS	Hybrid Synchronous
PCB	Printed Circuit Board
PM	Permanent Magnet
PWM	Pulse Width Modulation
RBF	Rotating-Bending Fatigue
S-N	Stress-Lifetime
UTM	Universal Testing Machine
VR	Variable Reluctance
ρ	Resistivity
A	Area
S_{Nf}	Fatigue Strength
L	Length of the Material
R	Resistance

1 INTRODUCTION

The 3D printed auxetic cell-based compliant gripper proposed and tested in the work by Netzev et al. [1] provides encouraging results towards implementing a robust blind grasping system suitable for (semi-)automated collaborative robotic applications. Compliant grippers composed of flexible auxetic cell structures are effective at blind grabs for complex shaped objects, thus reducing operational complexity arising from integrating gripper switching, and computer vision. Its design and structure allow for the delicate handling of fragile objects by distributing the applied force over multiple contact points. This gives the compliant gripper an advantage over traditional planar parallel grippers due to its ability to handle objects of varying shapes and sizes. However, manipulation of grasped load poses challenges in the industrial application of this gripper.

One way to improve component performance is to improve its design and fabrication characteristics to prevent accidental failure of components under stress. This is achieved through running stress tests on the mechanical component until failure [2]**.** Fatigue testing comes in different types and forms, each aimed at testing some specific characteristic(s) of a test piece. Choosing the right kind of test is the first step for carrying out such analyses. [3]

In the case of the 3D printed auxetic cell, the structure needs to be compressed to closure and then released to return to its resting position, repeatedly. This can be accomplished by conducting a constant amplitude stress test where the load is applied to the component in cycles until it breaks down [3]. By studying the behavior of the structure and the material under test, design decisions can be made to improve component performance and reliability [11].

While many commercially available machines can perform such tests, it is financially unfeasible to employ them for non-commercial testing meant for academic researchers and hobbyists. The price tag, along with the complicated setup, safety, and infrastructure demands of hydraulic and pneumatic actuators commonly used for generating loads in these machines, motivates the designing of a low-cost solution tailored towards non-industrial applications of fatigue testing machines (FTMs). [4]

1.1 Motivation

The 3D-printed auxetic cells designed by Metodi et al. [1] for their compliant gripper solution have proven effective at gripping parts of different shapes and sizes. However, these 3D-printed parts are prone to deterioration. It is mentioned that no fatigue has been observed during the 609 grasps performed during the gripper testing [1]. However, as the primary purpose of the auxetic cell-based gripper is undergoing repeated elastic stress, it is important to subject the device to a much higher number of stress cycles (>10,000) to study its durability and performance characteristics [14]. Therefore, the auxetic cells need to be subjected to high-cycle fatigue testing [11]. These tests provide useful data such as fatigue strength, fatigue life, and fatigue limit of the test specimen. This information can be used to improve the design and properties of future iterations of the auxetic cells. However, commercially available FTMs can cost upwards of a hundred thousand euros [6] and are cumbersome [4]. They also require additional safety and operational infrastructure. For testing this compliant cell, a custom-made testing rig consisting of easily accessible parts is the more economical and prudent approach.

1.2 Justification and Hypothesis

The thesis hypothesizes that a cheap and easy to assemble fatigue testing rig for the cyclical load can be used to test components easily without the use of expensive commercially available machines and the infrastructure required for them. Such a system can be set up using 3D printed parts, electrical actuators, and sensors.

1.3 Problem Statement

A fatigue testing machine capable of performing constant amplitude uniaxial load testing for auxetic cells needs to be designed that is economical and constructed with easily accessible parts and components. It should be able to test auxetic cells made from different materials, such as thermoplastics and steel. Sensors to detect force and displacement might be required. A torque of up to 70Nm is required based on the minimum possible component rigidity machined from steel. The idea is to create a cost-effective fatigue testing rig that is easy to assemble and control using electrical actuators.

1.3.1 Research Questions

- What are the issues with conventional fatigue testing solutions?
- What are the important design and configuration considerations?
- What can be improved/modified to meet requirements?
- What previous research has been conducted on this topic?
- How feasible is the proposed solution for the required testing?
- What are the shortcomings?
- Can it replace conventional fatigue testing machines?
- What materials and parts(motors/sensors) and design decisions could improve the proposed setup?

1.4 Scope

This thesis includes research in the field of fatigue testing machines, their structure, working principles, type of actuation and load testing, and the sensors and computation needed to read the data and turn it into information. This information is then used to create a setup that can perform similar tasks but is made from cheaper parts and requires minimum maintenance and is simple to assemble. The research also includes a case study which strengthens the findings of the thesis.

1.5 Challenges and Limitations

Using commonly available DC motors is cheap but comes with tradeoffs such as lower cycle frequency and available torque when compared to traditional hydraulic or pneumatic actuation. Considering the scope of this thesis, which is concerned with testing an auxetic cell machined out of steel that requires a stroke size of 5mm due to its design and dimensions, a low cycle frequency of around 0.5 Hz, and a torque requirement up to 70Nm, these tradeoffs are acceptable, and the use of motors can be justified. However, for other scenarios dealing with different components and materials, higher frequency constraints, and larger stroke sizes, modifications would be required in the proposed design that match the desired output. For example, a servo motor setup would allow for higher cycle frequency at a reduced torque but at the cost of greater system complexity, such as adding encoder circuitry, due to the feedback requirement for correct position measurement.

Furthermore, since the rig uses 3d printed parts in its structure, it is likely to be less robust compared to commercial FTMs, which will pose design and construction limitations of its own.

1.6 Document description

The first chapter of the thesis briefly introduces the reader to the problem statement and explores the justification. It informs the reader of the motivation behind this research, the problem statement that the thesis aims to solve, scope of the study, and its limitations. The second chapter familiarizes the reader further with fatigue testing by exploring the history and development of studying fatigue failures, the contributions towards improving fatigue testing and analysis, and the role and importance of performing fatigue testing. The third chapter focuses on developing the research methodology to enable swift designing of a fatigue testing machine utilizing electromechanical actuation. It details the development of the approach taken to find the solution. The fourth chapter describes the stepper motor-based solution, the algorithms used, and the possibilities of the developed solution. This chapter also details upon work on Simulink simulation and TinkerCad for where the developed solution was prototyped, and the results were recorded and analyzed. The fifth chapter shows the research results, including some analysis from the simulation study and other ideas to validate the developed solution. Further, the chapter provides a conclusion to the research. It addresses the shortcomings of the research work and suggests possibilities of future work to build on the current simulation and develop a physical prototype to carry out further experimentation.

2 LITERATURE REVIEW

2.1 Introduction

Fatigue failures have had catastrophic consequences in the past, such as the collapse of bridges and large structures, explosions, and significant and minor accidents, resulting in loss of human life [2][5]. Hence, it is crucial to study fatigue characteristics for all applications, particularly in areas where human collaboration is necessary. Elongating the lifespan of any component that comes under cyclic loading is a design issue that must be considered [10]. Pook et al. [11] highlight the vital role and positive impact standardized acceptance fatigue testing has played in improving the safety and quality of human life. A clear example of the advantages is the drastic reduction of fatigue failures in motor vehicles, which were quite common only a few decades ago [11].

2.2 Overview of the Phenomenon of Fatigue

Lee et al. describe fatigue as a "localized damage process of a component produced by cyclic loading" [8, p 57]. It is the failure of a component, structure, or machine due to the repeated exposure to constant or fluctuating stress for some number of times. This cyclic loading produces plastic deformation at the high-stress area, resulting in permanent damage [8]. A single load, far below the yield strength of a structure or component, is harmless. However, the same load causes extremely tiny fractures, which accumulate over time with repeated loading. After collecting sufficient damage, the part fails due to fatigue [5]. Ninety percent of all mechanical component failures occur due to fatigue [3].

Fatigue has been observed and studied as a phenomenon for over 170 years. Historically, it dates back to the 40s of the 19th century, when repetitive damage of rails was observed in the rail industry [9][13]. Before the 20th century and the advent of computers and other powerful instruments and mathematical tools, fatigue was considered an engineering problem since there was no way to observe the microscopic fractures in a component's structure [3][5]. Now, it is understood to be a material and design phenomenon [3].

August Wohler, regarded as the founder of fatigue strength testing [13], led the initial forays into investigating fatigue failures through fatigue testing [4]. His work provided concrete evidence of repeated stress, much lower in magnitude than the yield strength, leading to cracks and failure [13]. The S-N curve commonly used to describe stress fatigue is called the Wohler curve [3][4]. However, August Wohler had no contribution towards plotting a graphical representation of his gathered data [13].

Although August Wohler's work is inconsistent with the current knowledge and understanding of fatigue failures [13], it lays the foundations for this field of study. Since then, regular contributions have been made to add and improve methods and models of fatigue testing and analysis to provide more accurate fatigue life predictions [8][10][12][16][18]. The research work performed by Liu et al. [18] acknowledges these milestones. It attempts to provide new fatigue failure models for asymmetric cyclic stressing on materials exhibiting cyclic softening or hardening, which had not been considered previously. Furthermore, in their literature, Santecchia et al. [10] and Lee et al. [8] also provide references to contributions made by different teams of researchers in the field.

Over time, the prevention of fatigue failures has become an integral part of industrial, automotive, aircraft, and other engineering fields [4]. All manner of structural designs have strict requirements for safety [4], and as Pook et al. [11] discuss in their review of product standards in Britain, most of them require acceptance fatigue testing. Market forecasts expect continuing growth in demand for fatigue evaluation equipment [17]. Multiple factors are responsible for this surge, including the use of new technologies and the improvement of existing ones. Furthermore, the changing requirements for material durability, sustainability, and quality control is also a key reason [17].

Despite the growing body of research and understanding on the topic, predicting damage due to fatigue remains a complex problem [8]. This complexity is partly due to the other conditions that can play a part in the fatigue failure of a component. In their research, Gbasouzor et al. [2] show that, in addition to the magnitude of the load, such failures are affected by multiple factors such as temperature, atmospheric conditions, cycle frequency, and the external, internal defects on the test subject. Another reason is the introduction of new materials and innovation in technologies as they get broader adoption in industries such as aerospace, automotive, construction, etc. [4] [17]. Hence, it is impossible to use any prediction model as universal [10] and generates accurate predictions [2]. Therefore, all possible influences should be considered to mitigate the associated risks [2], and as pointed out by Banavasi et al. [4], continuous

and regular revision of engineering design and practices are necessary to keep up with the introduction of new materials, design concepts, and use contexts.

2.3 Fatigue Testing Methods

Defining the type of fatigue testing method helps to formulate the solution required to perform the testing. Fatigue tests are classified as high-cycle and low-cycle. High-cycle fatigue tests are characterized by load amplitudes in the elastic regime leading to minor plastic deformation and a high cycle count to component failure [8]. Conversely, low cycle fatigue tests utilize larger stress amplitudes that cause plastic deformation in each cycle, resulting in faster component failure [14].

Further classification between these methods is generally based on the nature of the test coupon, the objective of the test, and the type of stress administered along with its amplitude [3].

2.3.1 Constant-amplitude test

In this type of test, the specimen under stress is subjected to a load of non-varying amplitude. The load is applied and removed in cycles. The amount of stress applied can differ between different test components but does not change within a test cycle. Such tests can be further broken down into routine, short-life, and long-life test classes determined by the size of the stress amplitude utilized. This is the simplest method for conducting a fatigue test [3] and, as noted by Pook et al. [11], is commonly used for standardized component testing.

2.3.2 Variable-amplitude test

These tests aim to simulate real-life service stress profiles for the object under test. Stress amplitudes during a single test run are modified using simple or complex sequences. When a more straightforward arrangement is used, the resulting test is called the cumulative damage test. A test that applies more complex stress profiles to mimic real service load scenarios is called the service simulating test. [3]

2.3.3 Classification based on the nature of the test piece

Another approach to classifying fatigue tests is based on the nature of the component under test. Test pieces can be divided into specimen and component classifications. Specimen pieces are generally small, standardized, final products that allow for more control over the quality and characteristics of the product, thus mitigating some factors that might influence its fatigue performance. Results from these tests help in research

and provide data to improve the material and its fatigue properties. Component testing is similar to specimen testing but also includes factors such as the design, fabrication, assembly, and manufacturing of the test piece. [3]

2.3.4 General Classification of Fatigue Testing

Fatigue tests can also be categorized based on the objective of the test. The three categories are as follows:

Structural type test

This category tests between components made using different designs, fabrication processes, and materials to determine the integrity of their structure. The insights gained from these tests can help to inform on design and fabrication improvements while also narrowing down appropriate material options for the product. [3]

Material type test

These tests subject a test piece made from different materials to compare their performance when put under repeating stresses. It provides comparisons on the effects and behaviors of materials exposed to varying environmental conditions such as temperature, pressure, humidity, medium, etc. that the test piece may be subjected to during its operation. Moreover, it can also test the effect on fatigue properties of materials due to the surface treatment applied to them such as casehardening, nitriding, decarburization, etc. [3]

Actual service type test

Similar to variable-amplitude testing, these tests expose the test piece to real-world situations in terms of stress amplitudes and the expected environmental conditions to implement quality or reliability testing. [3]

2.4 Classification of Fatigue Testing Machine

Fatigue testing rigs come in various configurations to handle the varying demands for types of stress, test materials, operation characteristics, load magnitude, and other specifications and properties required for testing the subject. The two major classes for FMTs are based on the type of stressing method, and the type of actuation utilized for applying the load. Selecting the appropriate machine is important for achieving the objectives of the test. [3]

2.4.1 Classification Based on Type of Stress

- Rotating-Bending Fatigue (RBF) Machine

The RBF test is the oldest type of fatigue test, which uses a motor that applies torsional stress at different points on the surface of the test specimen. A stationary force supplied to a rotating sample causes the pressure at any point on the specimen's outer surface to travel from zero to maximum tension stress, back to zero, and then to compressive stress. This machine's S-N curve is described as a rotating-bending, stress-controlled fatigue data curve. A fixed stationary force is delivered to the specimen resulting in a constant bending moment that leads to fatigue failure. The motor moves with a constant frequency. To create a failure on the specimen, a constant-stationary force is applied to the specimen, which makes a constant bending moment [3]. Figure 1 shows a schematic drawing of an RBF machine.

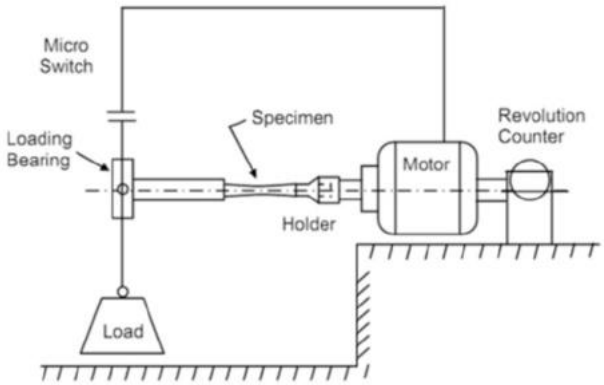

Figure 1 - RBF Machine Schematic [21]

The RBF testing machine constructed by Banavasi et al. [4] uses an electric motor as the stress-producing element and a system of pulleys and levers to transmit the load to the workpiece.

- Universal Testing Machine (UTM)

Universal testing machines are multi-purpose devices capable of exerting different types of stress over different materials to test their mechanical properties. These machines can individually exert compressive, tensile, rotational, or other kinds of forces as required from the machine. Azeez et al. [3] conduct their research on designing and analyzing a servo-hydraulic actuation-based UTM.

2.4.2 Classification Based on Stress Source

Azeez et al. [3] mention the following list of stress source types employed in fatigue testing.

1. Mechanical deflection
2. Deadweight or constant spring force
3. Centrifugal force
4. Electromagnetic force
5. Hydraulic force
6. Pneumatic force

When selecting the load generating source, it is essential to consider specifications such as frequency, the magnitude of forces, available control system, cost, and the accuracy of work environment simulation. [3]

2.5 Basic Components of a Fatigue Testing Rig

The core components of a fatigue testing rig are outlined by Banavasi et al. [4] in their work on designing a fatigue testing rig for various types of metals. According to this research, a fatigue testing rig consists of a load-producing mechanism, a load-transmitting mechanism, a counting device to track stress cycles, a power mechanism, and a frame [4]. Similar research work [2-7] on the design of fatigue testing rigs supports the same even though their implementation may differ depending on the nature and objective of the test. The rotating-bending fatigue testing machine constructed by Banavasi et al. [4] uses an electric motor as the stress-producing element. Azeez et al. [3] describe the fatigue testing machine in their work as a universal testing machine that has servo-hydraulic actuation for producing stress loads. Quadir et al. [5] have designed a reverse axial loading machine that uses an electric motor to generate fatigue loads. Henseler et al. [6] discuss the advantages of using a stepper motor to provide the load for its fatigue testing application. Jurecki et al. [7] also design their fatigue testing machine for testing metal bearings and opt for electro-hydraulic actuation as their stress source.

The load transmission is accomplished using a combination of pulleys, joints, guides, or grips that deliver the desired form of stress and its distribution to the test piece. Banavasi et al. [4] use a system of pulleys and levers to transmit the load to the workpiece as torsion and bending forces for their machine. Similarly, Quadir et al. [5] also use a pulley mechanism for load transmission in their fatigue tester.

A counting device keeps track of the cycles of stress applied to the workpiece. In combination with the power apparatus, the counter can shutdown testing after a required number of cycles have been achieved or on the occurrence of fatigue failure or deformation [3]. Gbasouzor et al. [2] employ a digital counter for this purpose which outputs the number of cycles based on the revolutions of a motor and terminates the test upon reaching the required value.

Finally, the frame of the machine is the structure that houses all the components of a testing rig, ensuring secure and stable functioning of the device and reducing vibrations during operation to mitigate its effects on the results. [3]

2.6 Fatigue Analysis Models

The stress-lifetime (S-N) curve plots the stress applied to a specimen against the number of cycles endured to failure. Figure 2 shows a typical plot of the S-N curve. The amplitude of the applied load is plotted against the total number of cycles on a log scale. This graph is a common method used to determine the fatigue properties of a material such as fatigue strength, fatigue life, and fatigue limit [14].

Fatigue limit defines the maximum stress that a material can endure without experiencing fatigue failure [14]. Fatigue life gives the number of stress cycles that a specimen can endure at a given stress level until it fails. Finally, fatigue strength (S_{Nf}) is the value of stress for a given number of cycles at which a component will fail. [14]

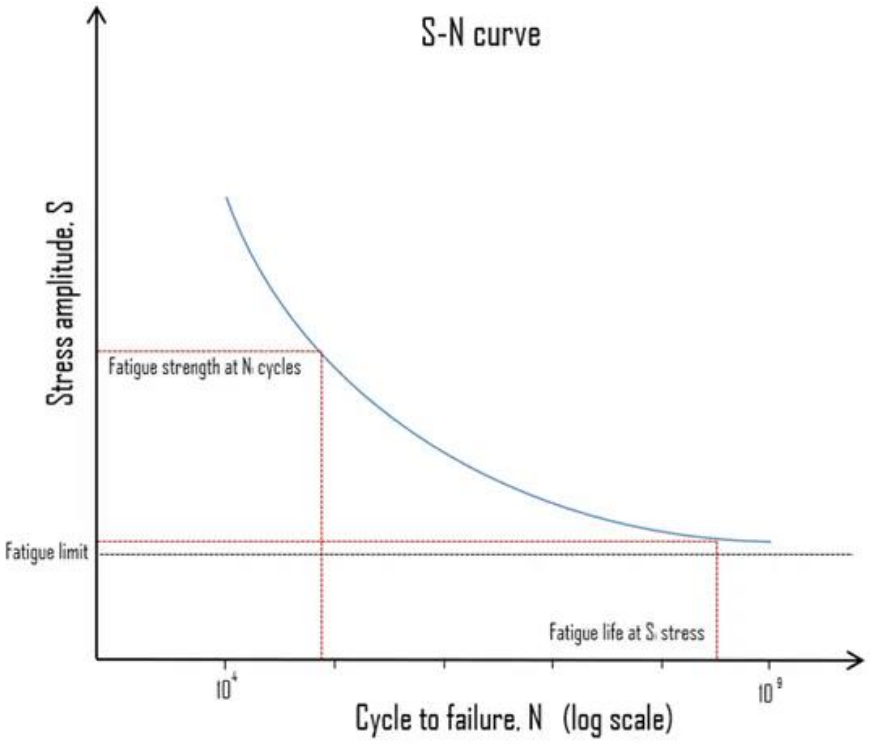

Figure 2 - S-N curve (Stress vs. number of cycles)

Fatigue failures, both for high and low cycles, all follow the same basic steps: the process of crack initiation, stage I crack growth, stage II crack growth, and finally ultimate failure [14].

According to Pook et al., component fatigue assessment is done in three main ways. These are the analytic approach, the standard design procedure approach, and service loading testing. Usually, a combination of these methods is required to produce meaningful results. Regardless of the choice of approach, it is vital to account for uncertainties and irregularities during service loads and scatter in the fatigue lives of components. [11]

2.6.1 High-Cycle Fatigue

High cycle fatigue requires more than 10^4 cycles to failure where stress is low and primarily elastic [14].

Many failure techniques have been developed in recent decades to correlate and predict the fatigue life of materials. Most failure models for high-cycle fatigue were developed using a stress-based approach, in which fatigue life was primarily connected to stress amplitude and mean stress.

The stress-life approach has traditionally been limited to high-cycle fatigue; however, recent research has shown that the stress-based approach can also correlate data from low-cycle fatigue. Instead of stress amplitude and mean stress, applied maximum stress and stress ratio are two essential variables in the stress-based failure models. [18]

2.6.2 Low-Cycle Fatigue

Low cycle fatigue tests feature high-stress amplitudes that cause repeated plastic deformation, and therefore, the number of cycles to failure is low. In the plastic region, significant changes in strain can be produced by small changes in stress. Failures that occur in lower than 10^4 cycles are categorized as low-cycle fatigue failures [14].

2.7 Counting Cycles

To plot the S-N curves generated by fatigue test results, the number of cycles needs to be tracked as the tests are executed. Gbasouzor et al. [2] use a digital counter for this purpose. The digital counter is a terminating device that gives out the equivalent value of the number of revolutions of a motor in terms of cycles. Fatigue tests that run for a long time must have the number of cycles recorded. To make the counter easy to use, a push button on the device allows quick resetting of the display count to start a new test. [2]

Tracking cycles for constant amplitude fatigue tests is a straightforward task. When the amplitude of the loading fluctuates over time, however, determining what defines a cycle and the matching amplitude becomes more challenging. [8]

Lee et al. [8] provide a comprehensive list of techniques that are utilized for situations where the test amplitudes variate with time. These are broadly categorized as one parameter, and two-parameter cycle counting techniques. The workings of these approaches are beyond the scope of this thesis.

2.8 Sources of Actuation

Fatigue testing machines come in a variety of stress source options [3]. Hydraulic, pneumatic, and servo-hydraulic loading mechanisms are common due to their reliability and speed of operation. While these modes of actuation have their benefits, they also add to the complexity and cost of the machine [4-7]. Jurecki et al. [7] conclude that this expense and complexity is acceptable for their application but in the work done by Henseler et al. [6], Quadir et al. [5], and Banavasi et al. [4] the expensive actuation

source has been replaced with electrical motors. The next sections provide a comparison between stepper and servo motor options, both of which can be utilized for fatigue testing applications [6].

2.8.1 AC vs. DC Motor

AC Motor

AC motors are cheaper and easy to drive/control.
They require low startup power and are highly durable, generate a higher torque and have a longer life span compared to DC motors.

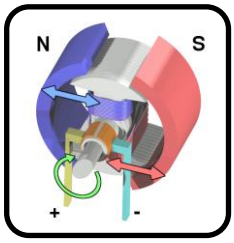

DC Motor

DC motors are more efficient and offer better responsiveness to control commands.
They have high startup torque and power with simpler installation and maintenance.
Suitable for current research since these are cheaper and easier to acquire

2.8.2 Stepper vs Servo Motor

Servo motors are not a specific category of motors but a combination of a regular AC or DC motor that is coupled with sensors and encoders to enable precise control of its angular position, acceleration, and velocity. The simplest servo motors use DC motors and a potentiometer to create a closed-loop servo mechanism. [20]

Stepper motors operate on pulses of direct current and move in discrete angular displacements called steps. These steps define the precision of the motor's movement. The number of poles available in the stator will determine the number and angle of each step [6] while the rotor is either a permanent magnet or made of a soft magnetic material [6][20]. Because of this structure, stepper motors are useful for applications that require precise motion without the added complexity for encoders. They also produce high holding torque at low speeds.

2.9 Sensors

Modern strain gauges are resistive devices that are used to test the load or strain that an object is subjected to. The resistance (R) measured in ohms in any resistance transducer is material and shape-dependent. The geometry is made up of the cross-

sectional area (A) along the length of the material (L), and the material's resistivity (ρ) is given as resistance per unit length area. [8]

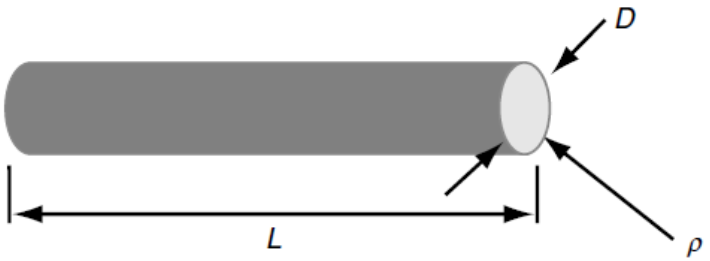

R = Resistance (ohms) *L* = Length *ρ* = Resistivity [(ohms × area) / length)]
A = Cross-sectional Area:
Area is sometimes presented in circular mils, which is the area of a 0.001-inch diameter.

Figure 3 - A simple resistance wire [8]

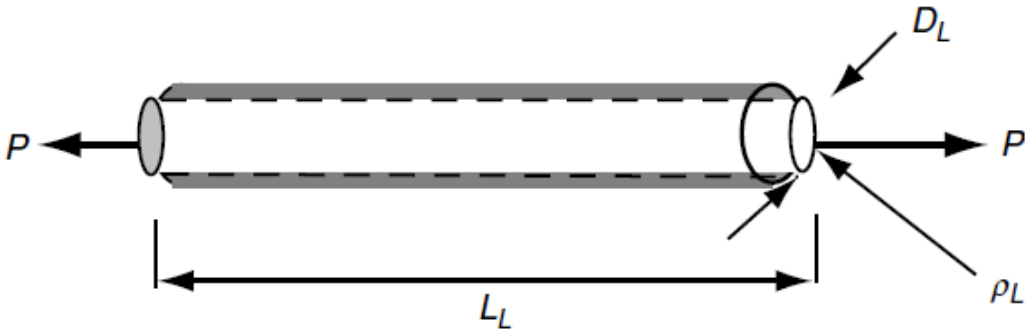

Figure 4 - A resistance wire under mechanical load [8]

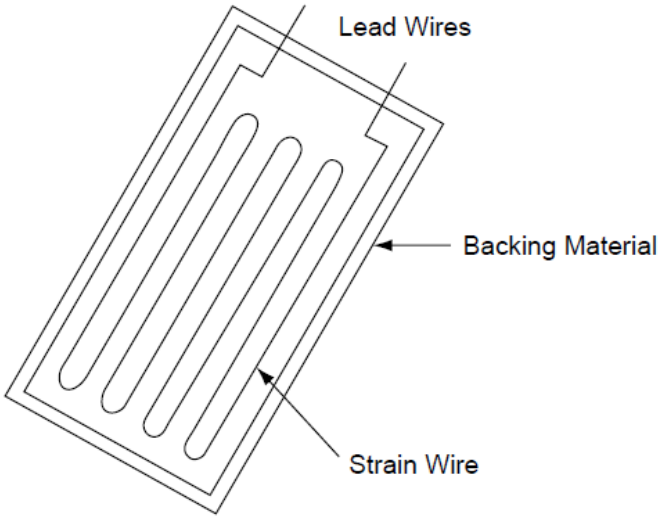

Figure 5 - A typical uniaxial strain gauge

Constantan is the typical material of choice from which such gauges are. The material used depends on the application, the material to which it is bonded, and the control required. [8]

Change in resistance of resistance strain gauge is directly proportional to the change in length per unit length experienced by the transducer. The wire gauge and the etched foil gauge are the two most common forms of strain gauges. [8]

The load cell has 4 strain gages inside wired in a Wheatstone bridge configuration. The strain gages are attached to the metal of the load cell, and they change resistance when loads deform the load cell. This change in resistance is much too small to measure directly with a multimeter. Therefore, it uses a Wheatstone bridge circuit, which can sense minute changes in resistance by measuring the change in voltage instead.

3 RESEARCH METHODOLOGY

Designing and construction of fatigue testing machines for fatigue research of materials continue to be of popular interest with the introduction of new materials and construction methods. With the proliferation of maker spaces as well as material testing in research, a surge in demand for FTMs has been observed [17]. While these machines are professionally built and reliable, commercially available fatigue testing rigs can cost up to hundreds of thousands of euros [6]. The hydraulic and pneumatic infrastructure requirements for powering these machines make them an unfeasible option for academic researchers and hobbyist groups [4].

Furthermore, the limited and basic functionality of these testing rigs [6] allows for creating economic alternatives that deliver satisfactory performances. As a result, the design and fabrication of low-cost machines capable of performing similar tasks have been the subject of research articles by Gbasouzor et al. [2], Banavasi et al. [4], Quadir et al. [5], and Jurecki et al. [7]. The literature review conducted for this thesis uncovered examples of FTMs with configurations designed to carry out different types of fatigue tests. As a result, previous research on this topic proved useful in defining the parts and components necessary for designing any fatigue testing machine.

In the research work produced by Henseler et al. [6], Quadir et al. [5], Banavasi et al. [4], Azeez et al. [3], and Gbasouzor et al. [2], the use of electromechanical actuation and control stands out as the cost-effective solution of choice that meets the requirements of conducting fatigue tests in maker spaces. However, to answer the research questions posited in section 1.3.1 above and address the problem statement, it is essential to consider the output requirements for the desired fatigue testing setup. A list of questions was identified to determine the core design characteristics of the electronics system required to drive the actuation mechanism.

3.1 Selecting the Motor Type

The motor type influences the selection of electronics and the microcontroller programming necessary to produce the required motion from the motor. Therefore, it is the first detail to consider and confirm before the system can be designed. It is commonplace to choose motors based on previous experience using them or the

comparative ease of driving them. Because of their robust and flexible nature, any motor may seem fit for a given task or operation. However, some key design features should make one motor type the ideal choice for a given application. This section will discuss a list of helpful questions for determining the right motor type for a given job.

The first detail to ascertain is the torque and force required from the motor for the fatigue application. This is determined by the magnitude of the load expected on the machine. The motor torque curve is consulted at this stage to check if it can deliver the required torque. The following property to consider is the revolution speed needed for the given torque range to provide the frequency demanded by the fatigue test. This is directly influenced by two factors, i.e., the properties of the mechanical system responsible for converting the rotational motion of the motor shaft into linear motion and the stroke size expected for the fatigue test. For this reason, this thesis work briefly discusses the gear systems that may suit the fatigue testing application despite the mechanical design of the FTM falling outside the scope of the research.

The nature of the load, i.e., whether the load remains constant or varies during the motor operation, also affects motor selection as some motors can handle changing loads during the process better than others. Another load characteristic to consider is whether it needs to be held in place or requires a specific holding torque. Finally, it is vital to consider the cost incurred by the chosen components. The price of a motor is determined by the quality of magnets and windings used in it. The running costs can also vary between motor types. The allocated budget determines the final system design and, therefore, its efficacy.

3.2 Choosing Motor Subtype

Once the selection of the type of motor has been concluded, there is another stage of selection to determine the subtype that would best suit the given application. Motors of the same type can come in various configurations, for example, stepper motors cam differ in the step count in a revolution, number of phases, number of poles, the type of wiring, and gearing. The combination of these characteristics determines the motor's output and performance and the components necessary to drive and control it. This also leads to differences in motor pricing. Once again, it is important to select the motor that fits the system requirements for performance and complexity while keeping within the given budget.

3.3 Environmental factors

Some types of fatigue tests simulate the environmental factors from the real-world operation of the test piece. In material type and service type fatigue testing, the specimen is tested under various environmental conditions [3]. Depending on the kind of fatigue test planned, conditions such as the medium of testing, i.e., in-air or submerged in water/liquid, temperature, humidity, pressure, and other such atmospheric properties impact the performance demands of the actuation system [2]. Therefore, it is essential to consider the environmental factors and the compatibility of the actuation source to these factors.

3.4 Motor Control Design

The components that make up a motor control system depend on the power requirements of the motor for the fatigue application and the type of motor to control. In its most basic configuration, a motor control system will consist of a controller, a driver circuit for the given motor, and the motor itself. While any controller is capable of driving a motor, regardless of its type, by using the appropriate programming, the driver circuit is unique for each type of motor and depending on the power requirements of the application, needs to be robust enough to handle large amounts of current if needed.

Additionally, a feedback mechanism can also be included in the control system. For some motors it is a compulsory addition that requires additional components and wiring and computation, thus increasing the system's complexity. For other types of motors, it is an optional component that can improve the system's performance but does not limit its function.

3.5 Mechanical System

The rotational motion of the motor needs to be translated in the desired form to the specimen being tested for fatigue. Depending on the type of test being administered, the motor is used to power the suitable mechanical setup. This can be a system of pulleys and/or an array of gears to produce the right movement in the load cell for the fatigue test. The required torque and stroke length also define the correct mechanical system for the job.

3.6 Force Sensor Interfacing

A combination of force sensors or strain gauges is used to measure the stress exerted on the test piece by the load cell during fatigue testing. The sensors are arranged in a wheat-stone bridge configuration. The generated output is amplified to improve the resolution of the sensors as it is fed back to the microcontroller for computation. Finally, the collected data is used to plot the S-N curve for the specimen under testing.

3.7 Simulating the Designed System

Before procuring the parts and components and assembling the designed actuation system, it is helpful to test it under simulated conditions to check if any shortcomings could potentially change the design. Simulating the system helps to verify the designed system. It saves time and money as the correct parts can be purchased in one go without having to change and reorder components if they fail due to a faulty initial design. There are a handful of useful tools available to academic researchers that can be used to model different parts of the electromechanical subsystems of a fatigue testing rig. Some simulation tools for electronics also provide the ability to burn the desired programming directly onto the microcontroller for practical testing. Once the simulation runs successfully and produces the desired results, it can be replicated on the physical setup without switching to different tools.

3.8 Conducting Practical Experiments

The final step of this framework involves taking the program running on the simulated microcontroller and running it on the actual microcontroller, and using it to run the motor and the mechanical system as designed. The initial testing versions can be set up using breadboards and jumper wires. This allows for easy adjustment of wires and components if some errors have been made in the connections, and also permits for quick replacement of parts if they fail during testing.

When the results and system performance has been verified, it is possible to move the simulated system onto a printed circuit board (PCB) to make it clean and permanent as the components are soldered onto the board. Once the circuit design is finalized, the pin connections can be transferred onto a PCB design software, and a CNC machine can produce the same circuit on a physical PCB.

3.9 Flowchart for the Framework

Using this line of inquiry combined with the information gleaned from the previous research on the subject of this thesis, an investigative approach has been developed to collect and compare the different viable options for the implementation of the required system. It is aimed at simplifying and expediting the process of designing an FTMs actuation system. The figure below describes this approach in the form of a flowchart. The idea is to formulate a comprehensive comparison that can simplify the process of selecting components when the output requirements for the FTM have been finalized.

Based on the literature review, a pattern emerged for the selection of motor actuators in the design of FTMs. Since these factors continue to guide the selection of motors in this research, it was felt that a concise matrix describing the best choice for FTM motors for the three parameters would simplify the process defined in the flowchart above. As motor selection is the first point of concern in the design of motor actuated FTM, having a system to easily identify the right motor for the job would streamline the whole process of designing the actuation system and save time. Therefore, a preliminary framework has been developed that compares motors for different ranges of torque, speed, and cost, which is delivered at the end of the next chapter.

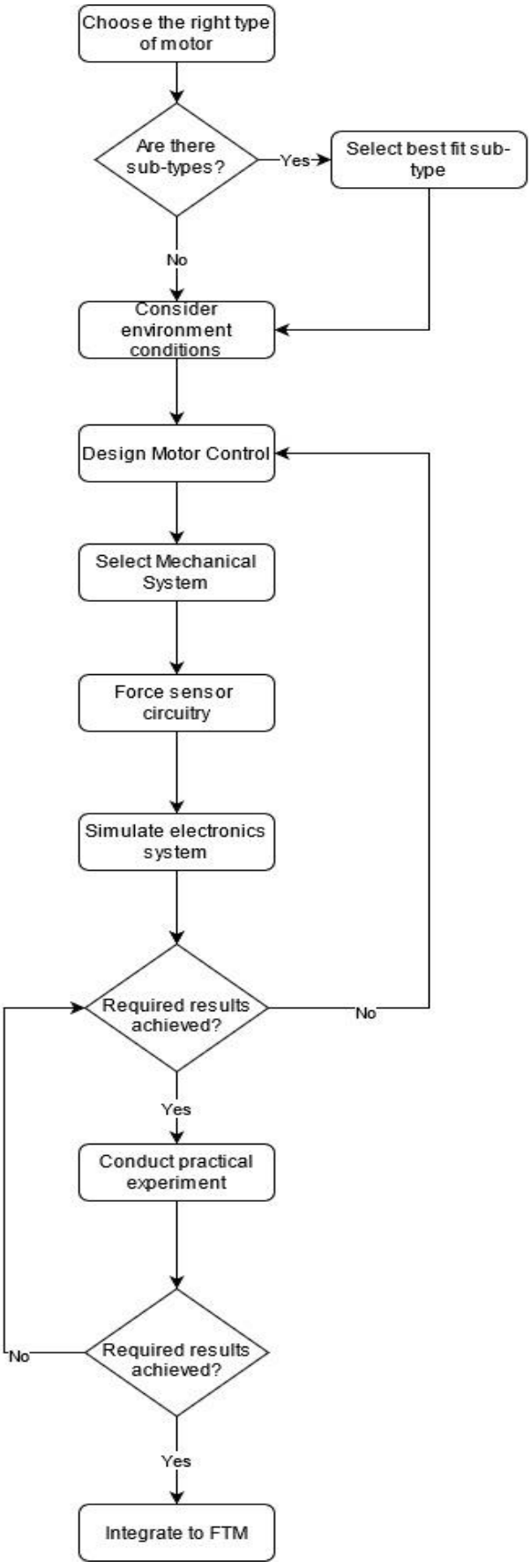

Figure 6 - Flowchart describing the steps required for designing an FTM using motors

The given directions can help identify components that will form the backbone of an electric motor-actuated FTM solution, with room for peripherals that enhance system functionality and performance at the cost of added complexity. The desired output of this thesis is to provide a simulation of the working of the motor controller circuitry that can be modified by providing parameters such as output force, frequency, and stroke size. Such flexibility in the actuation system would allow running different types of fatigue tests. The next chapter elaborates on the implementation of this research methodology.

4 EXECUTION

This chapter describes the complete implementation of the proposed solution. The research methodology defined in the previous chapter is put into practice, and simulations are performed to test the validity of the designed solution. As this thesis is more concerned with the electronics and computation domain, it does not detail the system's mechanical design. However, it was not possible to ignore the mechanical design as it has direct implications for motor rotation control. Hence, some reference designs have been studied. The primary circuit of the proposed configuration is implemented in Autodesk's TinkerCad environment. The relevant block diagram is given in Figure 35.

The work done shall also be helpful in understanding how to select the right configuration for a compression-based fatigue testing scenario for a similar or different test piece under variable environmental conditions while keeping in mind the cost of the whole system. This exercise shall be followed with a basic framework developed during this thesis for addressing the research questions mentioned in Chapter 1.

4.1 Environment Impact

The first step in designing the actuation mechanism is to consider the environmental properties the fatigue test needs to simulate. The uniaxial constant amplitude fatigue test does not expose the test piece to real-world operation conditions. Furthermore, the FTM being designed is to be used indoors at room temperature and pressure. Hence, there will be no external factors to consider in the system design.

4.2 Identification of the Motor type

As explored in the literature review, both the stepper motor and the servo motor system are possible options for the application of a fatigue testing actuator. To single out the appropriate motor type, we shall use the filtering approach defined in the research methodology. A suitable motor has to be chosen based on the application's requirements and the motor's operational characteristics. Stepper and servo motors differ in their construction and means of control [20]. The following table provides a comprehensive comparison between the two types of actuators.

Stepper Motor	Servo Motor
A stepper motor typically has between 50 to 100 magnetic pairs or poles [19] adding more granularity to its motion and hence, better positional precision	Servo motors usually have between 4 to 12 poles [19]
Stepper motors operate on pulses of direct current and move in discrete angular displacements called steps [6]	Servo motors can run on both AC and DC power [20]
The rotor in a servo motor is either a permanent magnet or made of a soft magnetic material [6][19]	They can supply double their rated torque for short bursts of time.
Stepper motors perform better on lower speed applications [19]	Servo motor provides constant torque regardless of its speed.
They operate on lower revolutions per minute and provide less torque at higher speeds [19]	They are capable of operating at higher speeds and can maintain torque at those speeds [19]
Higher phase count in a stepper motor can improve torque but the addition of phases adds to the complexity of the driver circuitry [6]	The need for driver circuitry adds complexity to the system [20]
Stepper motors are susceptible to vibration and resonance problems which can lead to the motor stalling, skipping steps, and excessive noise and vibration [19]	Positional control on servo motors requires rotary encoders to keep track of motor movement [20]

Table 1 - Servo and stepper motor comparison

From the analysis above, it's noted that the stepper motor can deliver a higher holding torque at lower speeds compared to a servo motor of the same size. This is also relevant for the next inquiry which is the required speed of operation for the application. A frequency of 0.5 Hz is required with a stroke size of 5mm for the end effector. The low cycle frequency combined with the small stroke size should be deliverable by a motor operating at low speeds, although this is also dependent on the mechanical design of the actuation mechanism.

4.3 Selecting the Motor Type

4.3.1 Torque Required for the Application

The FTM being designed is aimed at testing auxetic cells to be used in compliant grippers for blind grasping of objects [1]. Auxetic cells are soft and flexible, making them a valid option for use in soft grippers. The stiffness and conforming capacity of a soft gripper depend on the stiffness of the construction material. Auxetic cells can be manufactured using different materials to acquire the required properties for the compliant cell and the cell stack to be used in the soft gripper [2]. Hence, a torque of up

to 70 Nm has been defined to produce the required load to compress the auxetic cell machined from steel. This is a large value that is available in heavy-duty industrial motors for both the stepper and servo motors.

4.3.2 Required Motor Speed (Torque + Speed)

From the design properties of the auxetic cell, a stroke size of 5mm for the end effector is sufficient to compress the test specimen to closure. A frequency of 0.5 Hz for the cyclical loading of the test piece denotes a slow-speed operation. The frequency has been selected in an appropriate range to closely represent the operating speeds of auxetic cell-based grippers in normal working conditions [1].

The speed of a motor's rotation can impact its torque output. The low cycle frequency combined with the small stroke size should be deliverable by a motor operating at low speeds, although this is also dependent on the mechanical design of the actuation system.

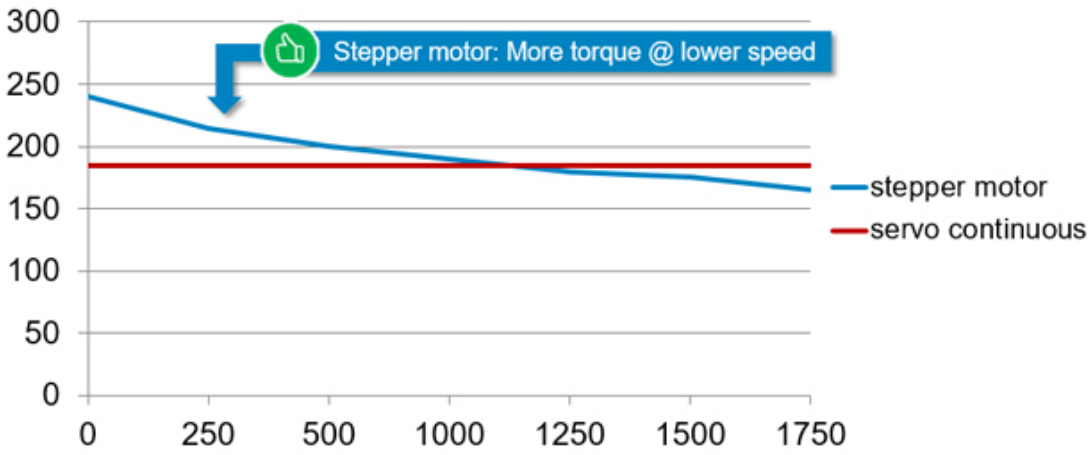

Figure 7 - Comparison of stepper and servo motor torque against RPM

From the analysis above, it's noted that the stepper motor can deliver a higher holding torque at lower speeds compared to a servo motor of the same size. At low speeds, the stepper and servo motors are both possible options. However, if a high load cycle frequency is required, the servo motor could be the better option to maintain its torque. In contrast, a stepper motor loses its torque output with the increase in its speed.

4.3.3 Load Characteristics

The structure of an auxetic cell allows it to deform with the application of a compressive force [1]. The force required to press down on the cell will be greater the further down it is compressed. Hence, during the fatigue test cycle, the end effector will experience a changing load as it moves from zero loads, when the compliant cell is in resting

position, to a peak load when the stroke reaches its maximum value, the cell is compressed to closure. Some motors are better equipped at handling changing loads during operation than others. A servo motor can boost its torque output for a few moments to overcome changes in load. In a similar situation, a stepper motor is incapable of increasing its peak torque. If the variation in load requires a torque higher than the stepper motor can generate at its speed of operation, it will lead to motor slippage resulting in skipped steps and loss of its position.

4.3.4 Special Functions: Holding Torque

If the auxetic cell needs to be held in a pressed state for a particular duration, a holding torque will be required to keep the end effector at that position. One example of this scenario is when the end effector pushes the piece down to closure, pauses, and then changes direction to release the applied load. Holding torques are a unique feature found in stepper motors because of how they operate in discrete steps. Servo motors require PID control to maintain their positional accuracy where the motor oscillates about the desired position. The error in the oscillation would depend on the accuracy of the PID control. Another way to maintain a servo motor's position would be through a mechanical design, e.g., a cam-follower mechanism like in Figure 8. However, such a mechanical solution requires a prescribed motion program that can only produce a fixed motion. A change in test configurations would require the construction of a new cam-follower design.

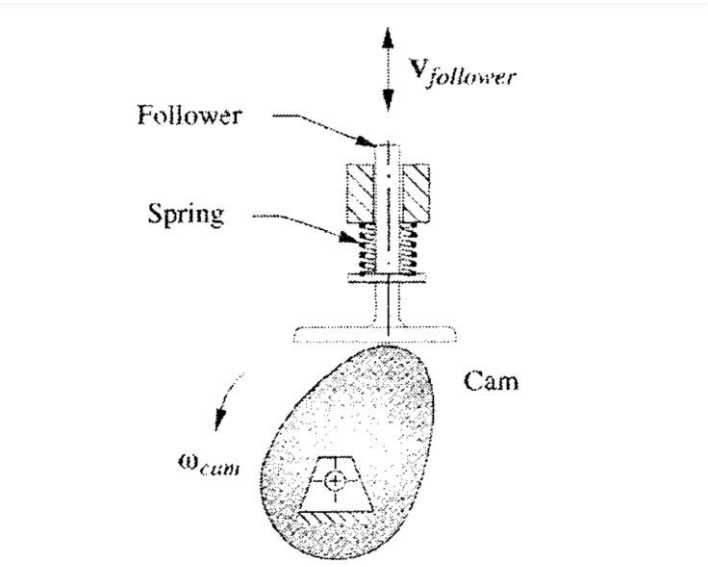

Figure 8 - Cam-follower mechanism [25]

4.3.5 Cost Overview

The problem statement for this research revolves around limiting the cost and complexity of the FTM. A major portion of the cost rises from the motor selected to power the actuation mechanism. Apart from the motor itself, the type of motor also incurs costs from the additional components required to run and drive it properly. Furthermore, these auxiliary parts add to the system complexity.

A stepper motor is a cheaper option than a comparable servo motor because it can function without a feedback mechanism, use cheaper magnets, and generally come without gearboxes. They are also cheaper to run as they can hold their position at zero current, thus consuming less power. On the other hand, a servo motor needs a feedback loop to work, uses expensive magnets, and often incorporates gearboxes. Moreover, they continue to consume power even at zero speed.

4.3.6 Decision on Motor Type

Servo motors are adept at handling varying loads by increasing the output torque to maintain speed. They are helpful in applications where torque remains constant at different rates of rotation. It is also possible to cap the torque generated by a servo motor by limiting its current. However, the stepper motor is cheaper to operate, can provide higher torque, and holds torque even at zero speed. The stepper motor is simpler to integrate into a circuit as it is easier to drive and does not need a feedback loop. It is also the cheaper of the two options.

From the detailed comparison performed between a stepper and servo motor, it is safe to conclude that overall, stepper motors are suitable for low-speed and high torque applications [6] [19]. The stepper motor is a better fit for the desired FTM application than a servo motor considering the requirements for a cost-effective and straightforward actuation system and the high torque range.

4.4 Choosing Motor Subtype

Stepper motors come in three main types, i.e., variable reluctance (VR), permanent magnet (PM), and hybrid synchronous (HS) motors.

The VR motor has a plain iron rotor, while the PM utilizes a permanent magnet instead for its rotor. An iron rotor makes the VR more robust due to its simple construction, but it also means that the motor cannot provide holding torque without being powered [24]. VR motors can also mitigate torque loss at higher speeds and are functional even at rates higher than 10,000 steps per second. Hence, in applications where the HS and

the PM motors would require gearing, VR motors can be used without gearboxes [24]. Finally, a VR motor is generally moved in full-step increments, whereas the HS and PM can also run on half-step increments, producing a smooth, jerk-free motion. Figure 9 shows the rotor and windings of the VR motor.

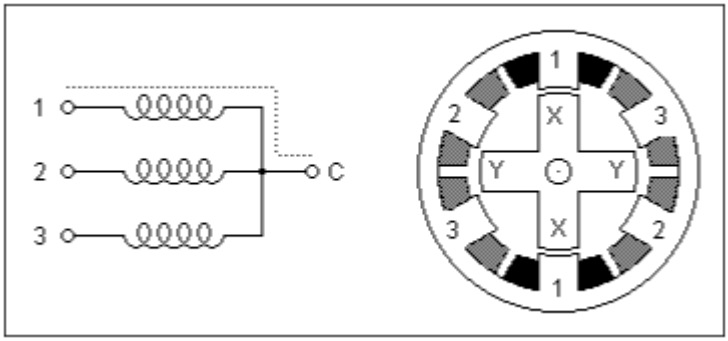

Figure 9 – VR stepper motor rotor and windings setup [24]

On the other hand, PM motors are the least costly option of all motors [24]. The HS motor has the permanent magnet of the PM motor and the stator poles of the VR motor. These configurations allow the HS motor to have a higher torque-to-size ratio, higher output speeds, and a smaller step size than other stepper motors [6]. It is possible to use the same driver circuitry and wiring for a PM, and an HS stepper motor, making them interchangeable. The key differences between a PM and HS motor are resolution and cost. PM motors generally come in step sizes of 30 to 3.6 degrees with more than 50 magnetic poles. With finely cut teeth at the end cap of the motor's rotor, it is possible to get a step size of 1.8 degrees as well. While HS motors can have higher step rates than a PM motor, they will generally lose torque output when operating above speeds of 5000 steps in a second [24]. HS motors also suffer from vibration noise [24].

Stepper motors also come in unipolar, bipolar, or multi-phase combinations. A higher phase count translates to lower vibration levels and a higher power density and increases expenses. Furthermore, the addition of phases adds to the complexity of the driver circuitry. Choosing between a unipolar or bipolar drive system rests on drive simplicity and power to weight ratio. For a unipolar stepper motor, a simple single transistor circuit for each winding can drive the motor. Bipolar motors require an H-bridge configuration of transistors, although it is possible to use premade driver ICs available in the marketplace. Bipolar also provide approximately 30% more torque than a comparable unipolar motor because they energize the whole winding during operation. In comparison, a unipolar motor only energizes half of a winding at a time. [24]

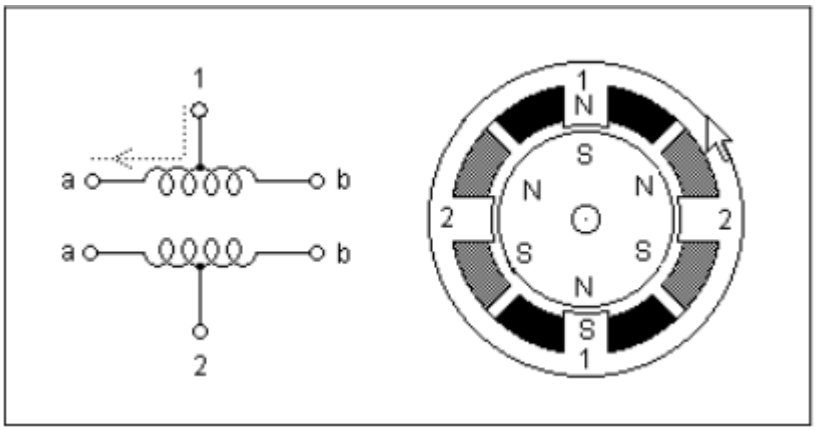

Figure 10 - Unipolar stepper motor rotor and winding setup [24]

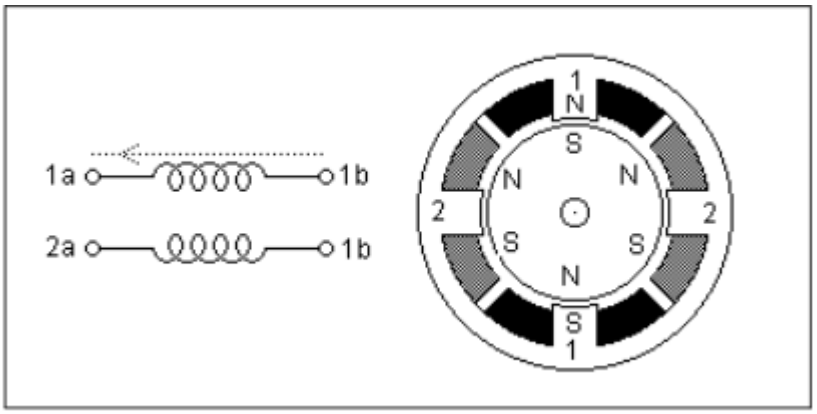

Figure 11 - Bipolar stepper motor rotor and winding setup [24]

A hybrid bipolar stepper motor utilizes a permanent magnet and a variable reluctance stepper to generate high torque output with smaller step angles [24]. Considering the torque, speed, and accuracy requirements of the FTM, this type of stepper motor would be a good fit for the application.

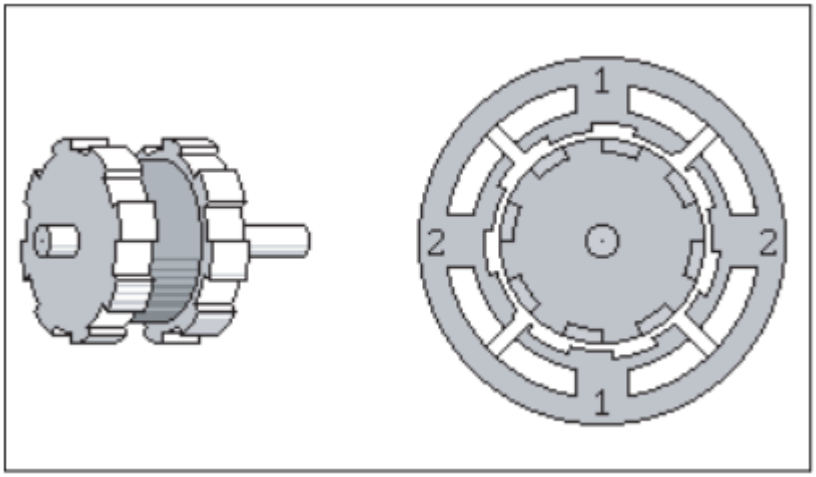

Figure 12 - Hybrid stepper motor [24]

4.5 Motor Control Design

The components that make up a motor control system depend on the power requirements of the motor for the fatigue application and the type of motor to control. In its most basic configuration, a motor control system will consist of a controller, a driver circuit for the selected motor. Any microcontroller can drive a motor, regardless of its type, by using the appropriate programming. The driver circuit will be unique for each motor type and, depending on the application's power requirements, needs to be robust enough to handle large amounts of current if required.

Additionally, the control system can include a feedback mechanism. It is a compulsory addition for some motors requiring additional components, wiring, and computation, thus increasing the system's complexity. For other types of motors, it is an optional component that can improve the system's performance but does not limit its function.

4.6 Mechanical System

The motor's rotational motion needs to be translated to the desired form for the specimen being tested for fatigue. Depending on the type of testing, the motor is used to control the suitable mechanical setup. This can be a system of pulleys or an array of gears to produce the proper movement in the load cell for the fatigue test. The required torque and stroke length also define the correct mechanical system for the job.

4.7 Force Sensor Interfacing

A combination of force sensors is used to measure the stress exerted on the test piece by the load cell during fatigue testing. The output from this circuit is amplified to improve the resolution of the sensors as it is fed back to the microcontroller for computation.

4.8 Simulating the Designed System

4.8.1 MATLAB/Simulink Simulation

MATLAB provides a Simulink simulation to control a bipolar stepper motor for speed or position. In the original model, the input signal is generated by a Step block, which produces a step signal with the required amplitude for the given set step time, followed by the required Final Value for the remainder of the simulation time. Depending on the

active control mode, i.e., speed or position, the initial and final step signal values are treated as steps per second, or steps with respect to the zero position, respectively. This input signal is fed into the controller block, which supplies the required pulse width modulation signal and the direction control for the bipolar stepper motor. The stepper motor driver block takes the output of the controller block. This driver block is a Simulink model implementation of an H-bridge IC to reverse the current flowing through the motor's phases. The driver takes care of energizing these phases in the required order to produce the desired rotation. A scope is connected to the output of the stepper motor, which monitors the shaft angle during simulation.

A subsystem simulates the required input parameters of speed and direction. Figure 13 shows this subsystem with the label 'Bidirectional Input Speed Control.' It uses pulse width generator blocks to produce the input signal to control the motor rotation. The subsystem is configured to create different movement patterns to express its flexibility for adapting to varying test scenarios. The following section details the subsystem and the workings of its inner components. The figure below depicts the stepper motor control model used for this simulation.

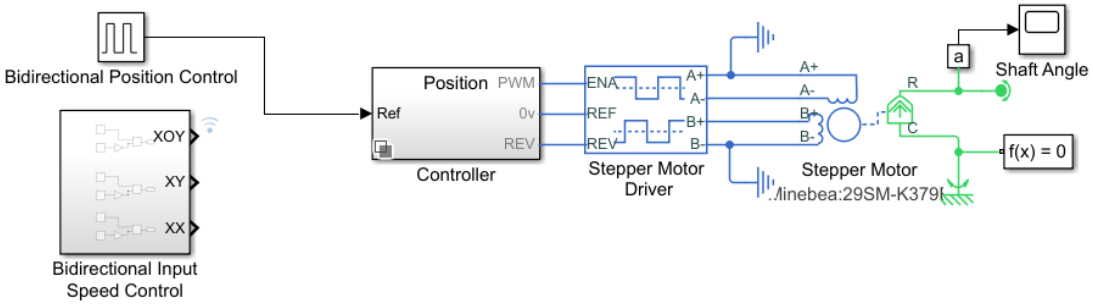

Figure 13 - MATLAB/Simulink stepper motor control model

4.8.2 Component Description

Input Signal Block

The input signal block is created to simulate the speed, position, and direction control inputs that would be programmed in a microcontroller in the practical setup of the FTM. There is no position control required for the unidirectional motion because the motor continues to rotate in the given direction throughout the simulation. Therefore, it has only been simulated for the speed control mode. The signal is generated using the step function block, which provides a continuous signal at the given amplitude for the desired step time, after which it changes to the given final value for the remainder of the simulation time. The step block parameters and their corresponding output signal for a simulation time of 20 seconds are shown in Figure 14 and Figure 15.

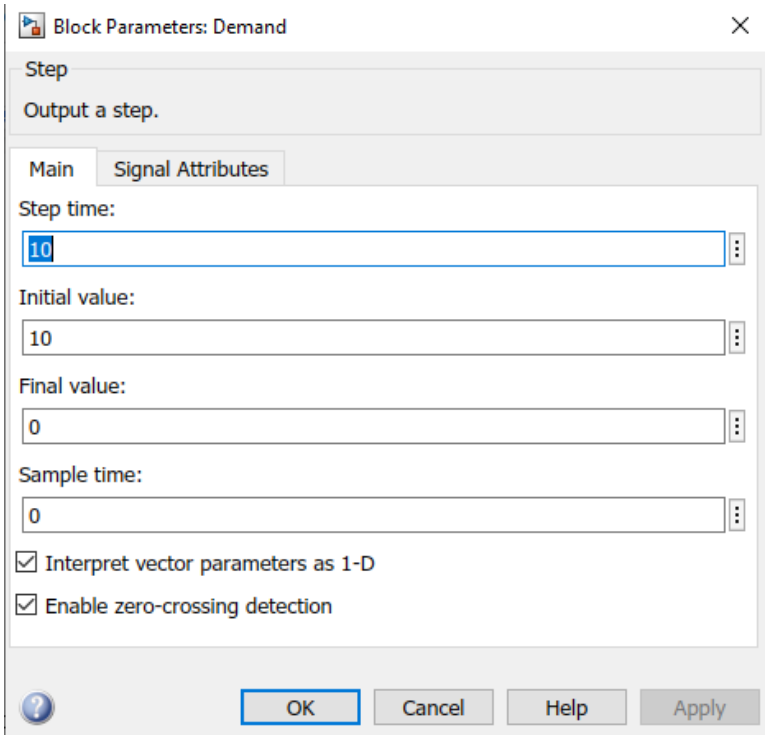

Figure 14 - Step signal generator parameters

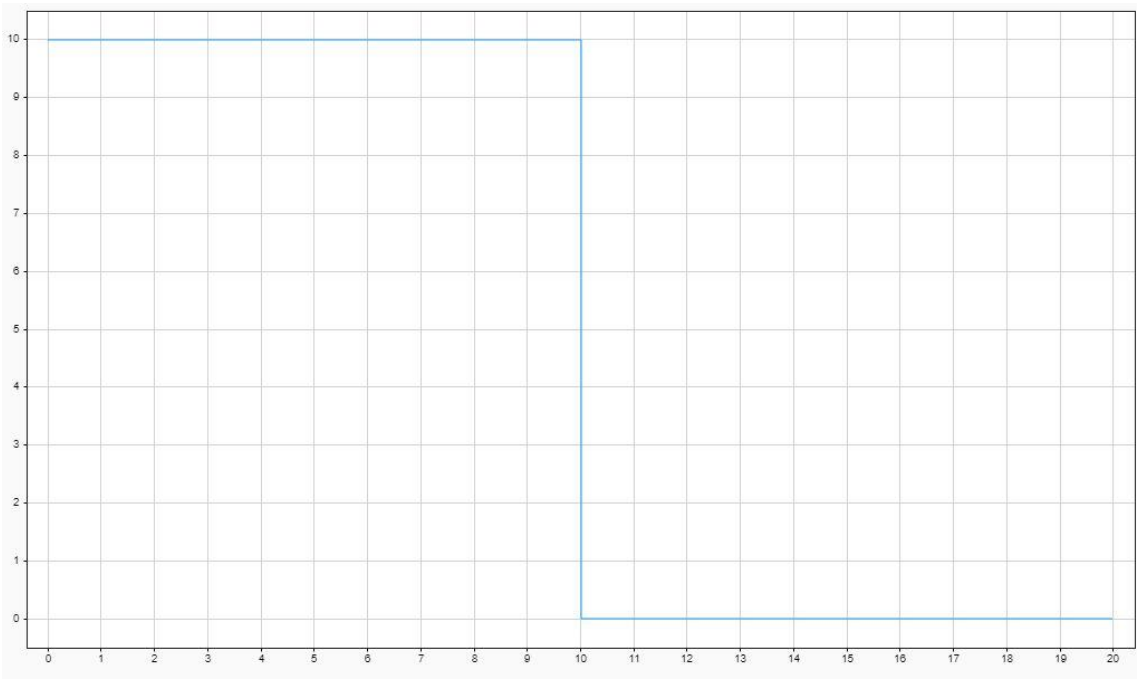

Figure 15 - Step signal generator output for parameters in Figure 14

Two types of input signal blocks have been used to deliver bidirectional motor control for speed and position control modes. A single pulse generator is sufficient for position control to move the motor shaft by the required number of steps and then bring them back to the zero position. The input signal for this operation is shown in the figure below, which cycles the motor rotation forwards and backward five steps for the entire simulation duration.

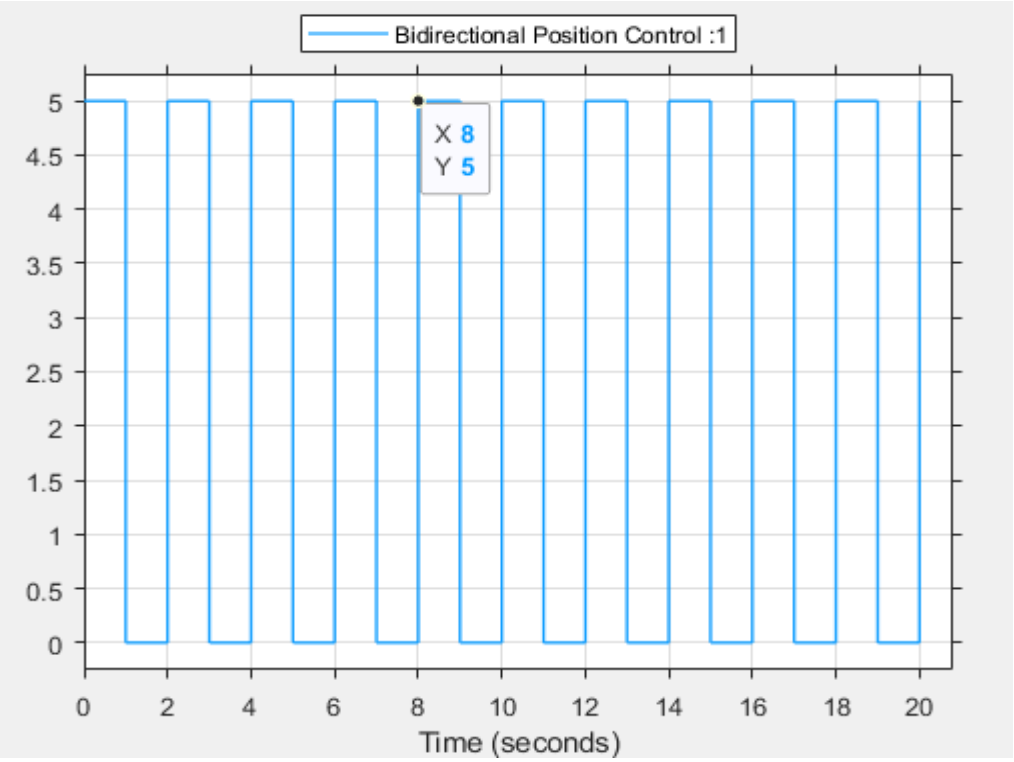

Figure 16 - Input signal for position control

The speed control input block provides three outputs to simulate three possible test scenarios. The outputs X0Y and XY produce two different rotation speeds during a cycle where X represents the forward rotation speed, and Y represents the backward rotation speed. In X0Y, a pause is added between rotations. XX represents equal back and forth rotation speeds. A combination of pulse generators and signal phase shifts are used to create the required outputs for these test scenarios. The inner structure of this subsystem is shown in Figure 17.

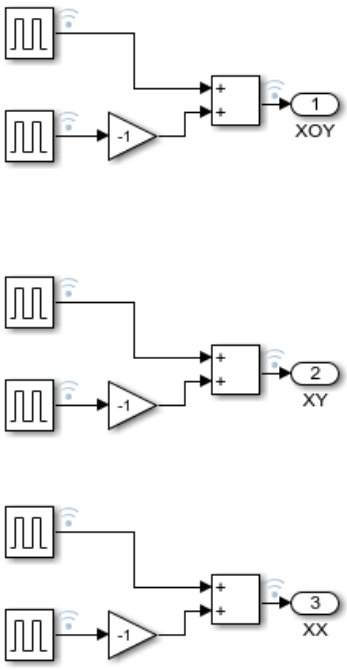

Figure 17 - Input signal generator model

Controller Block

The controller block takes the signal from the input signal block and generates the required pulse width modulation (PWM) and direction signals, depending on the active control mode. Figure 18 shows the inside of the control block with the position mode activated.

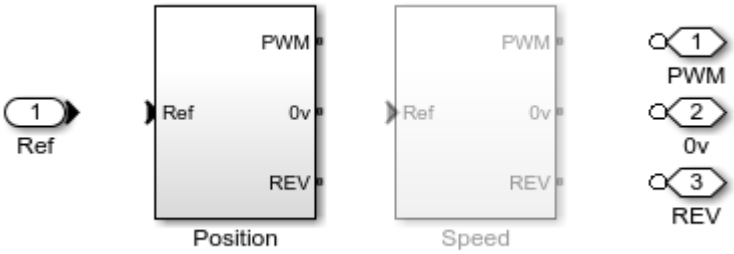

Figure 18 - Simulink controller block model

Further inside the position control resides the algorithm and pulse generation simulator. The speed, in terms of steps/s, at which this position control operates can be selected here. Figure 19 shows the block and a pulse rate of 5, which sets the stepper motor's speed at five steps per second.

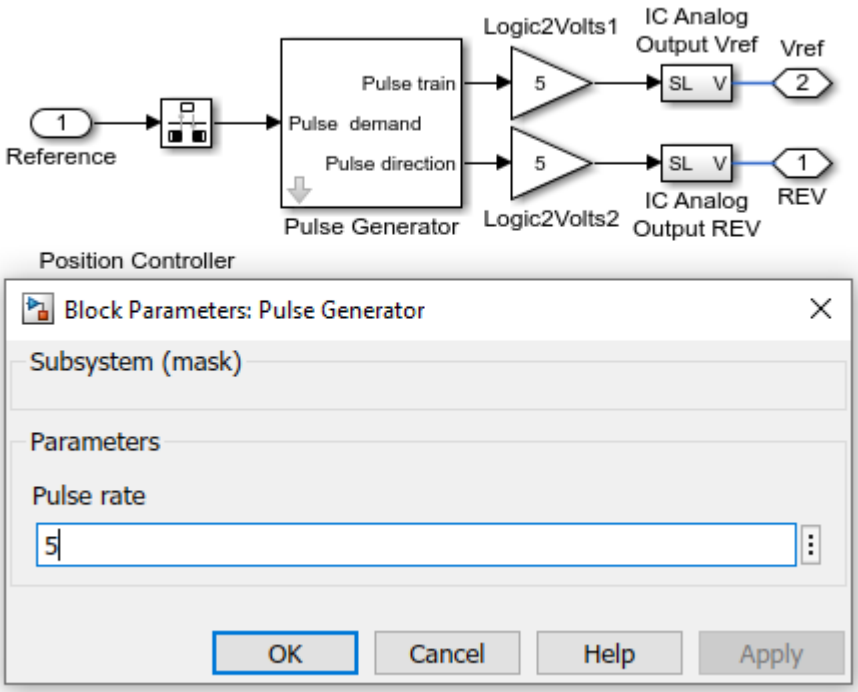

Figure 19 - Pulse rate parameter input for controlling motor speed during position control simulation

Stepper Motor Driver

The stepper motor driver block for a bipolar stepper motor represents the IC comprising transistors and diodes arranged in an H-bridge formation required to control the direction of the current flowing through the motor's phases. It also determines which phases are energized and their sequence. Figure 20 is a schematic drawing of the internal circuitry of the IC and how it uses the Input PWM signal to direct motor movement.

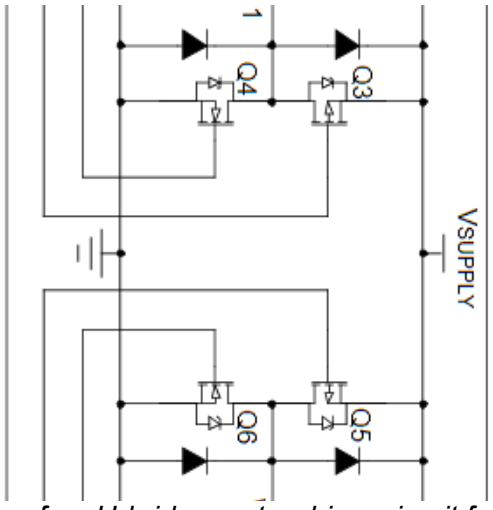

Figure 20 - Schematic drawing of an H-bridge motor driver circuit for a two-phase bipolar stepper motor [24]

In the Simulink block, the driver can be configured to move the motor in full-step or half-step movements. In full-step rotation, only one phase is energized, resulting in a step rotation equal to the step angle of the engine. In half-step mode, two phases can be energized simultaneously, and the sequence of energizing the phase can control the motor movement to a granularity of half the size of the given step angle for the motor.

Stepper Motor

The bipolar stepper motor block on Simulink allows the modification of its response characteristics by changing its parameters. Figure 21 and Figure 22 show the available parameter options, which can be changed to match any motor by using the appropriate values from its datasheet. This allows for a more accurate simulation of the motor response in a real-world application.

The block also provides a preloaded stepper motor selection menu for different makes and models of motors. This can be accessed by clicking the 'Selecting a predefined parameterization' option visible in the block parameters window in Figure 21. Selecting the motor will autoload its corresponding values and properties in the parameters window. The motor selection window is shown in Figure 23. Although limited in its selection, it is a convenient option to observe and compare different motor types.

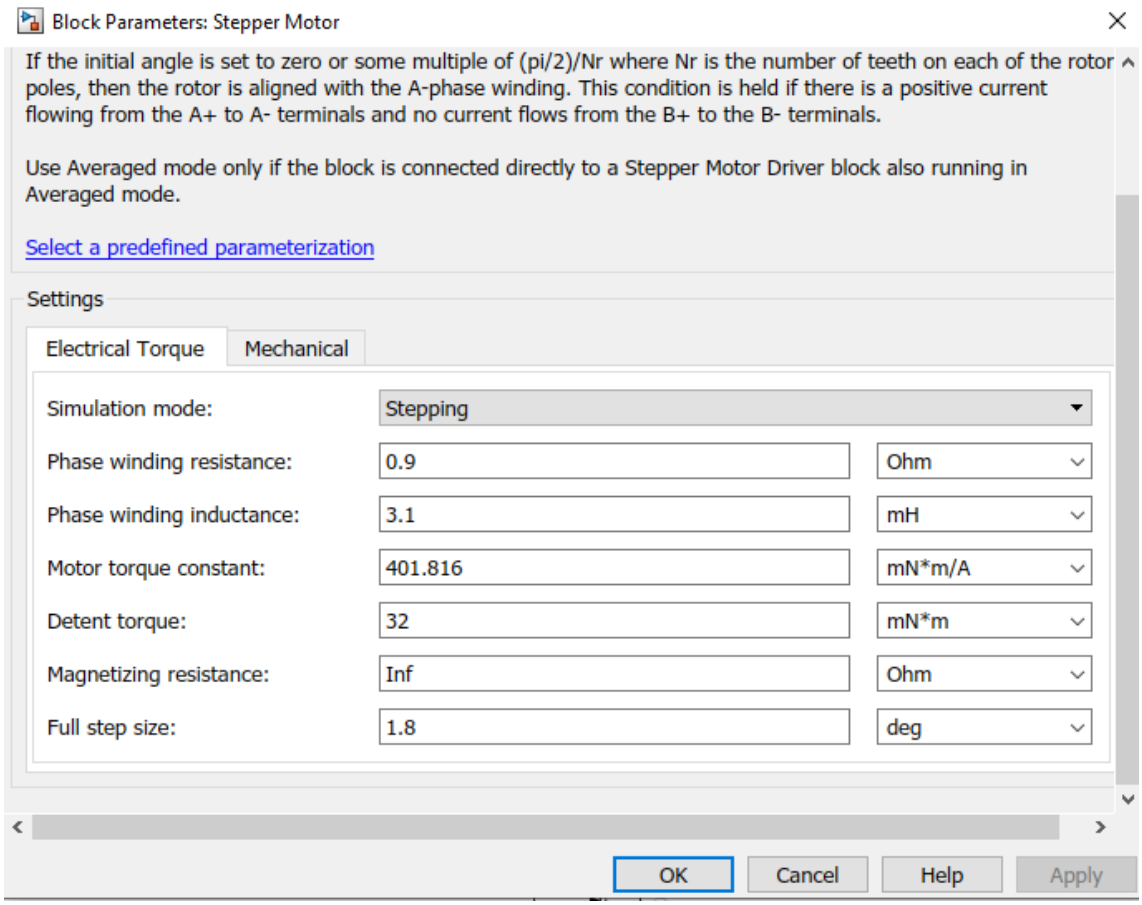

Figure 21 - Stepper motor model: electric torque parameters

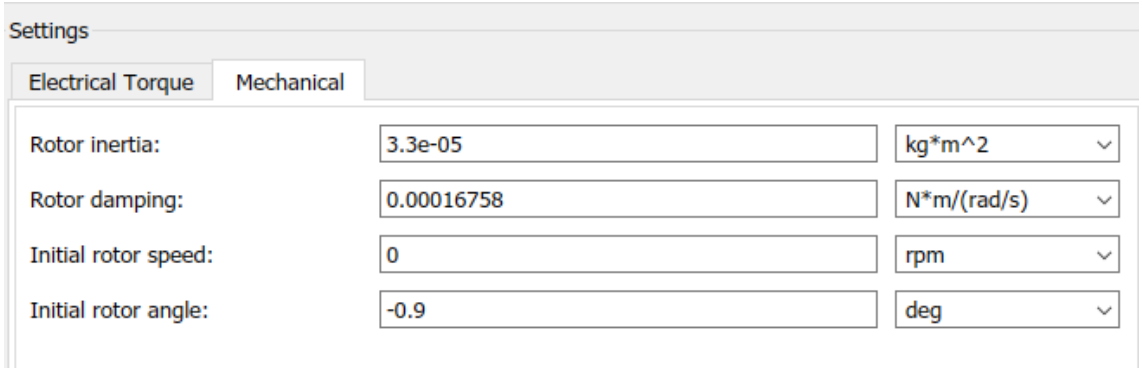

Figure 22 - Stepper motor: mechanical parameters

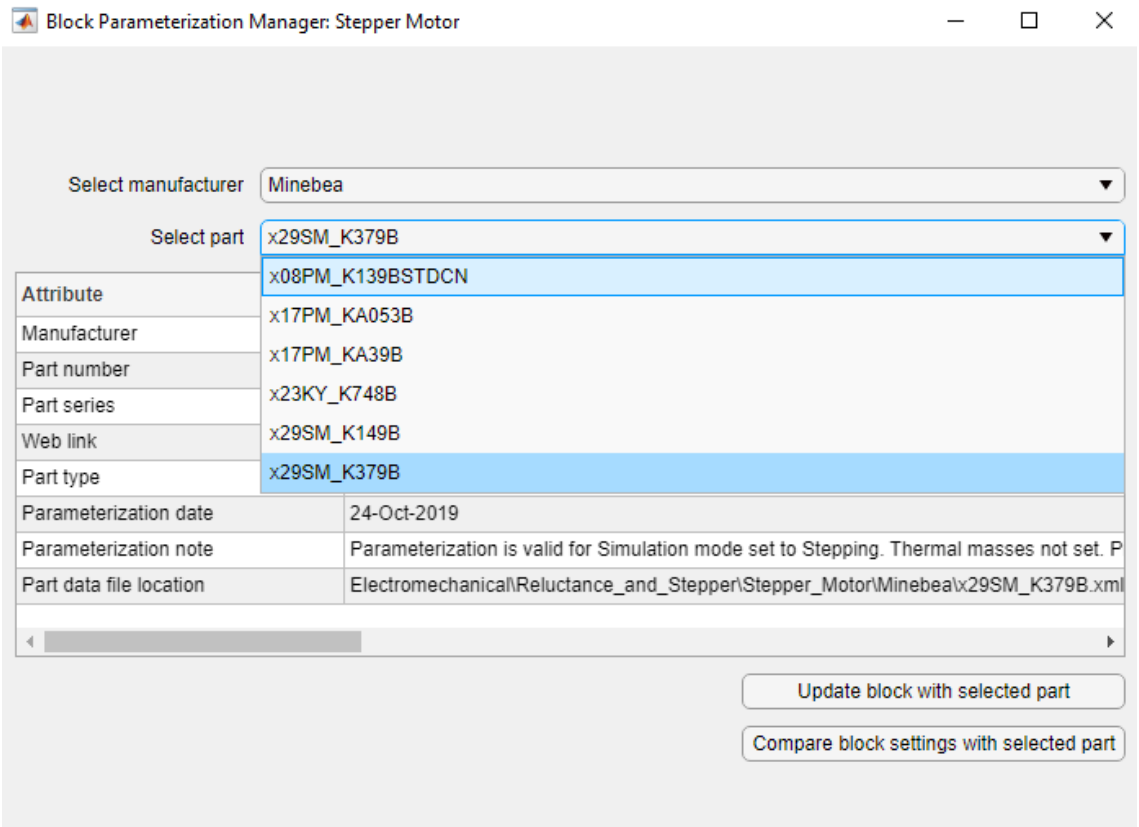

Figure 23 - Stepper motor models: preloaded motor model selection

The following sections explore a bipolar stepper motor simulation control using the position control and the speed control options.

Position Control

For the position control mode, the input signal delivered to the controller block gives the required step movement with respect to the motor's starting position. Hence, an amplitude of positive 5 of the input signals will move the motor five steps in the clockwise direction from step 0, and an amplitude of 0 from the input signal will cause the motor to return to its starting position. This behavior is explored in the position control simulation with an Input square wave signal with an amplitude of 5. The graph below shows the motor's response to the bidirectional position control input shown in Figure 24 for the first five seconds of the simulation.

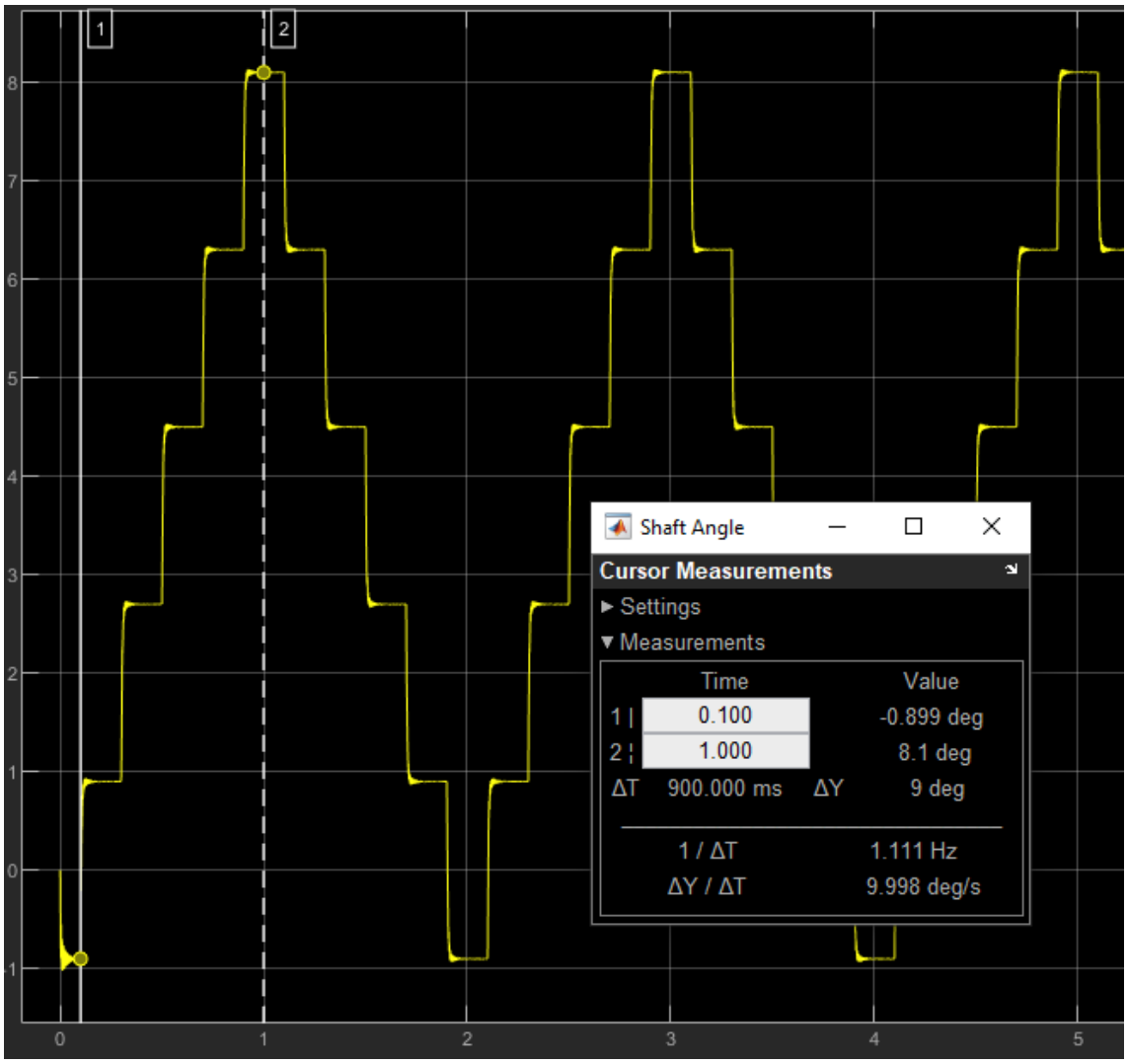

Figure 24 - First 5 seconds of bidirectional position control output (degrees vs. time)

Each complete cycle takes 2 seconds, giving a frequency of 0.5 Hz. The motor takes five steps in one direction per second, denoted by the plateaus in the graph. As discussed in the component description section of the controller block, this speed is fixed by setting the pulse rate for the pulse generator block depicted in Figure 15**.** The step angle for the motor is 1.8 degrees. It was noticed that the angle has an offset of about -0.9 degrees resulting in the maximum rotation of 8.1 degrees, as shown in the cursor measurement window. However, the total angle move comes out to 9 degrees. To correct this error, the initial rotation angle is set to -0.9 degrees in the mechanical properties of the stepper motor model. The output for the same input signal is shown in the graph below.

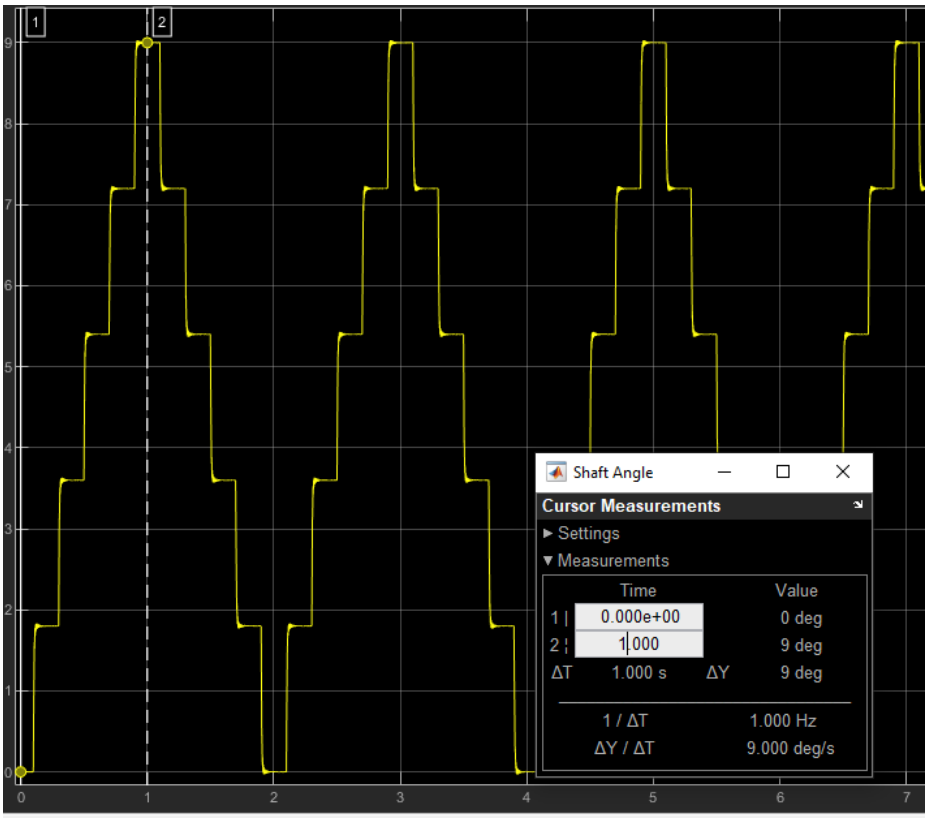

Figure 25 - Bidirectional position control output rotation (degrees vs. time)

The position control option is effective and simpler to control when the motor moves at the same speed during the forward and backward rotation. However, it cannot be simulated to drive the motor at different step rates for different directions. The speed control mode enables the speed of the motor to be varied at different parts of the motor's operation. This is done by manipulating the input signal to the controller block, as discussed above. The following section elaborates on the different test scenarios that can be simulated using the speed control mode.

Speed Control

The input is designed to create two types of test scenarios, one with only unidirectional rotation of the motor and the other with back and forth rotation to achieve the same angle of rotation at varying clockwise and counterclockwise speeds.

Unidirectional Rotation

A constant amplitude input signal that remains unchanged throughout the simulation time will rotate the motor in the same direction, with the amplitude equal to the speed of rotation required. Figure 26 shows the shaft angle movement plotted against time for the step input signal given in Figure 15.

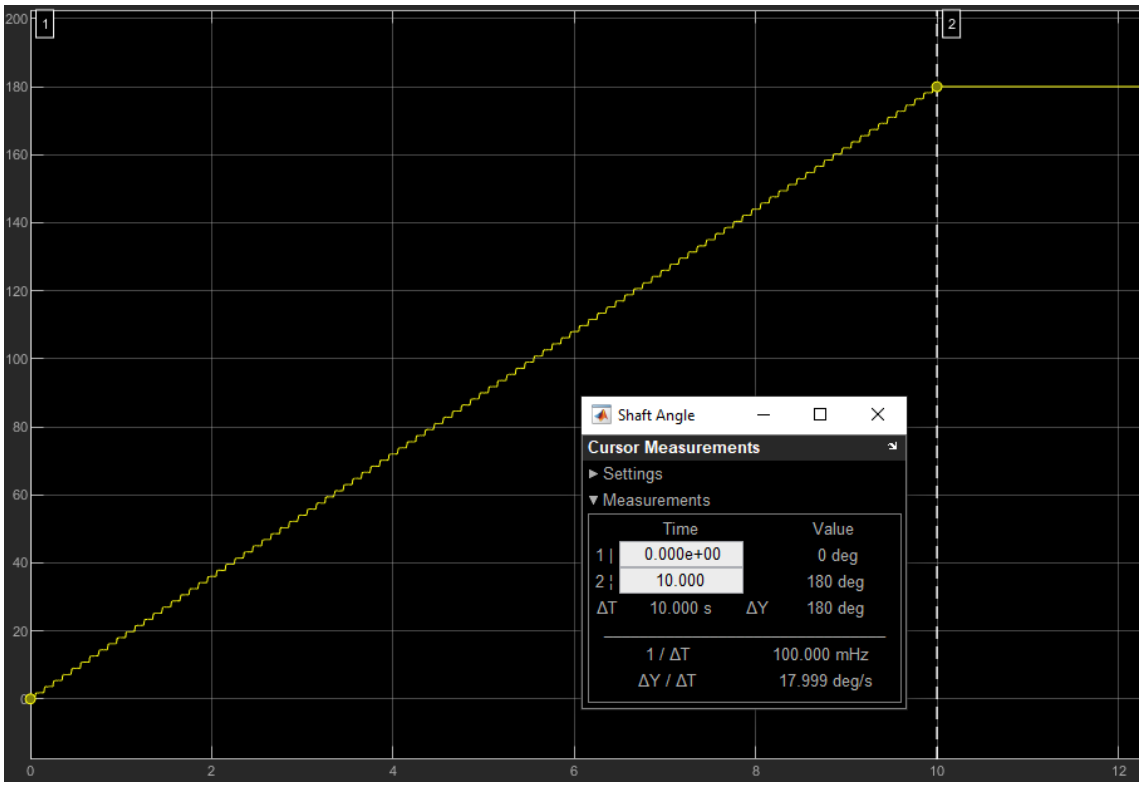

Figure 26 - Shaft angle plotted against time for unidirectional speed control

The input rotates the motor at ten steps per second for 10 seconds resulting in a total rotation of 180 degrees, each step being 1.8 degrees in size. The rotation stops as it gets an input of 0 steps per second for the remainder of the simulation time. Hence, the horizontal line at 180 degrees after the 10-second mark in the graph.

A variation of this test case could require changing the rotation speeds at different intervals of the fatigue test. The input signal is modified to jump to a different amplitude for the duration that requires constant amplitude testing at different speeds to simulate this variation. The graphs in Figure 27 and Figure 28 show the input and corresponding motor shaft rotation for this scenario plotted against time.

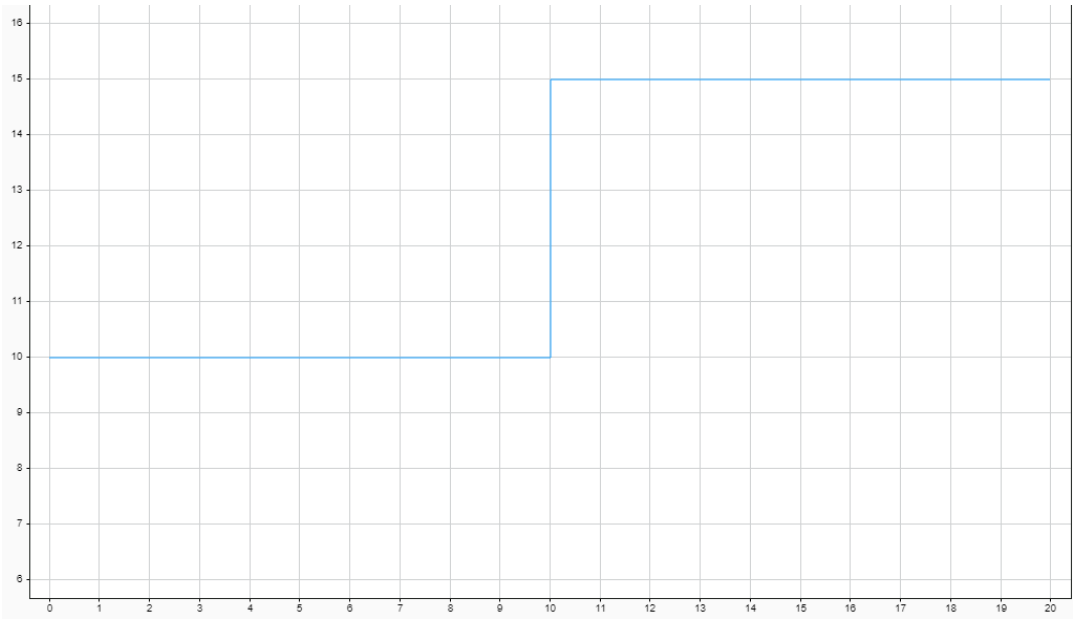

Figure 27 - Unidirectional multi-speed input signal

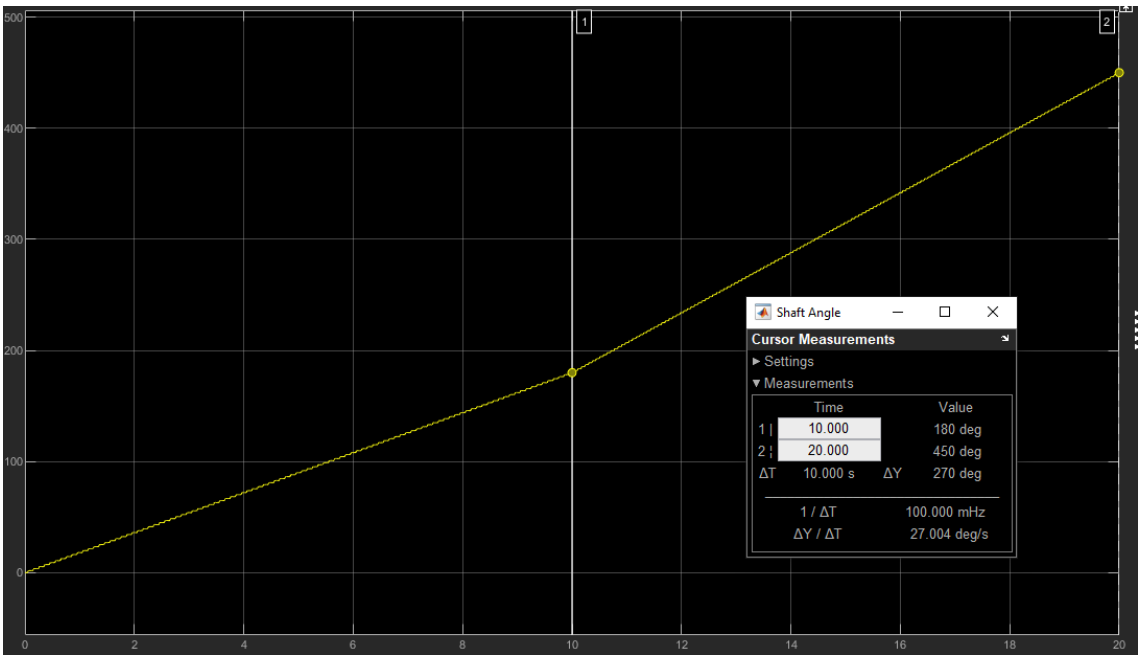

Figure 28 - Unidirectional multi-speed motor shaft output (angle vs. time)

The graph shows the motor rotating at ten steps per second for the first 10 seconds, reaching 180 degrees, followed by a boost in speed at 15 steps per second for the next 20 seconds, rotating a total of 450 degrees.

Such control would be helpful for an FTM which uses a cam-follower mechanical actuator to produce the required vertical or horizontal movement.

Bidirectional Rotation

Changing a motor's rotation would be necessary for mechanical systems, other than a cam-follower, converting rotation to linear movement. To simulate this movement, the input signal is switched between positive and negative amplitudes, the negative amplitudes corresponding to rotation in the opposite direction. Three test cases have been simulated based on different patterns of rotation that could be useful in a uniaxial constant amplitude fatigue test. These patterns and their control logic are explained below. X denotes the speed for stroke movement in one direction, whereas Y denotes the speed for the opposite direction to return the motor, and therefore the mechanical system, to its starting position.

X0Y

This version mimics a test case requiring unequal speeds for press and release motion of the mechanical actuator with a pause between the two movements, keeping the auxetic cell test piece closed for a small duration.

The input signal for this movement is formulated using a combination of two pulse wave generator blocks to create a signal that switches between three amplitude levels i.e. the amplitude of the two denoting clockwise and counterclockwise rotational speeds and zero to keep the motor at the required position. The two pulse waves have a phase shift to make the combined desired input signal for the controller block. This input signal and its simulation blocks are shown in the figure below.

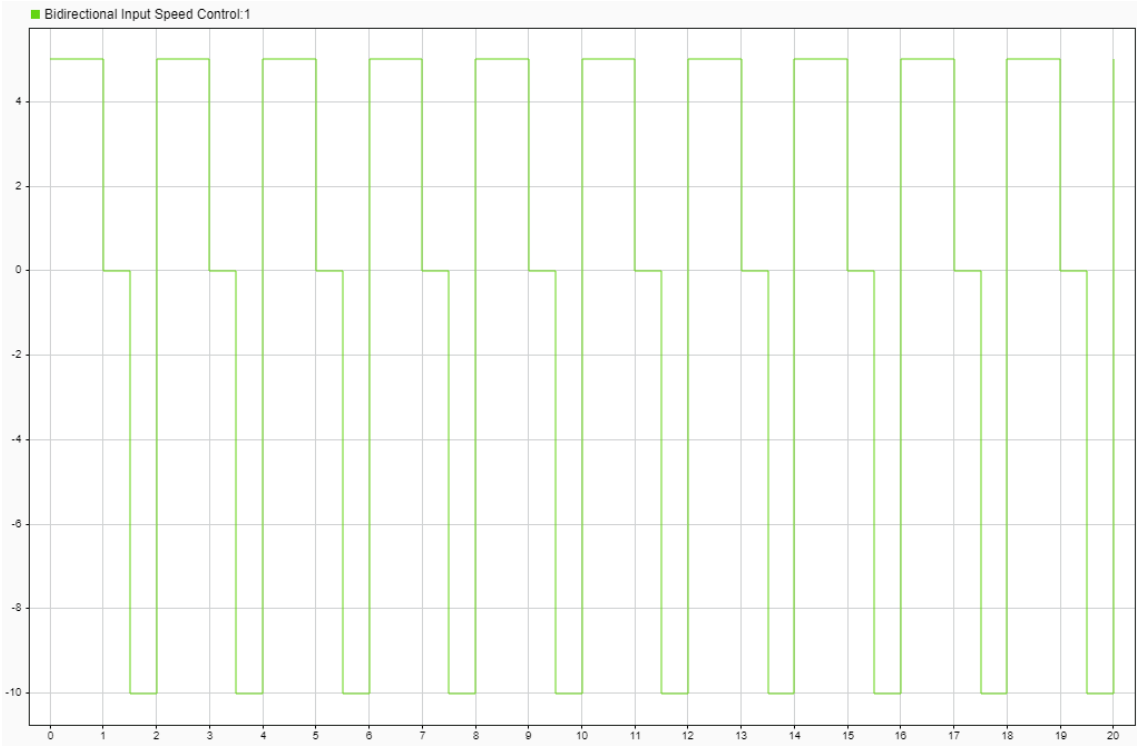

Figure 29 - Bidirectional speed control input signal for varying speed rotation

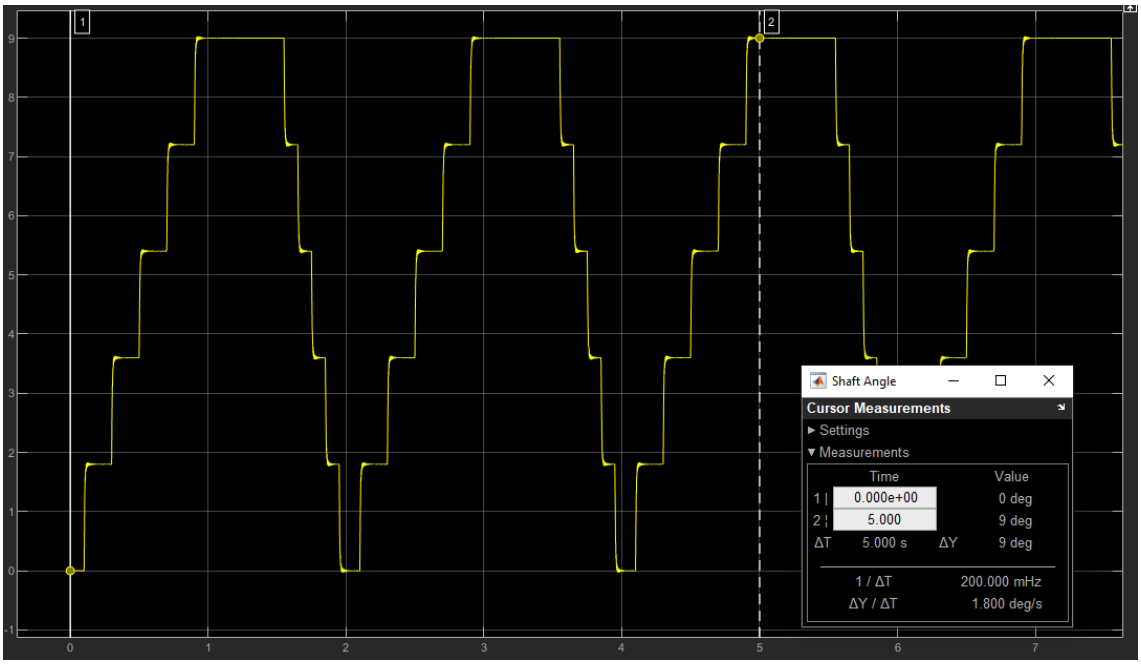

Figure 30 - Bidirectional speed control output for varying speed rotation (angle vs. time)

As depicted by the graph in Figure 30, the motor rotates in the positive direction by 9 degrees for 1 second, maintains this position for half a second, and rotates in the negative direction to return to its starting position in the next half-second. The shorter steps during the returning rotation denote the higher speed of the motor's rotation. The required speed for the forwards and backward rotation determine the amount of time

the input signal stays at the corresponding step level to achieve the number of steps necessary to bring the motor back to its starting point.

XY

In this test scenario, there is no pause in the middle of the stroke. The input signal switches between two amplitudes only, performing the backward and forwards movement at different speeds repeated throughout the simulation. As in the X0Y test case, the speed desired for the motor movement determines the amount of time the input signal continues at the given amplitude. The input signal and its corresponding output are shown in Figure 31 and Figure 32, respectively.

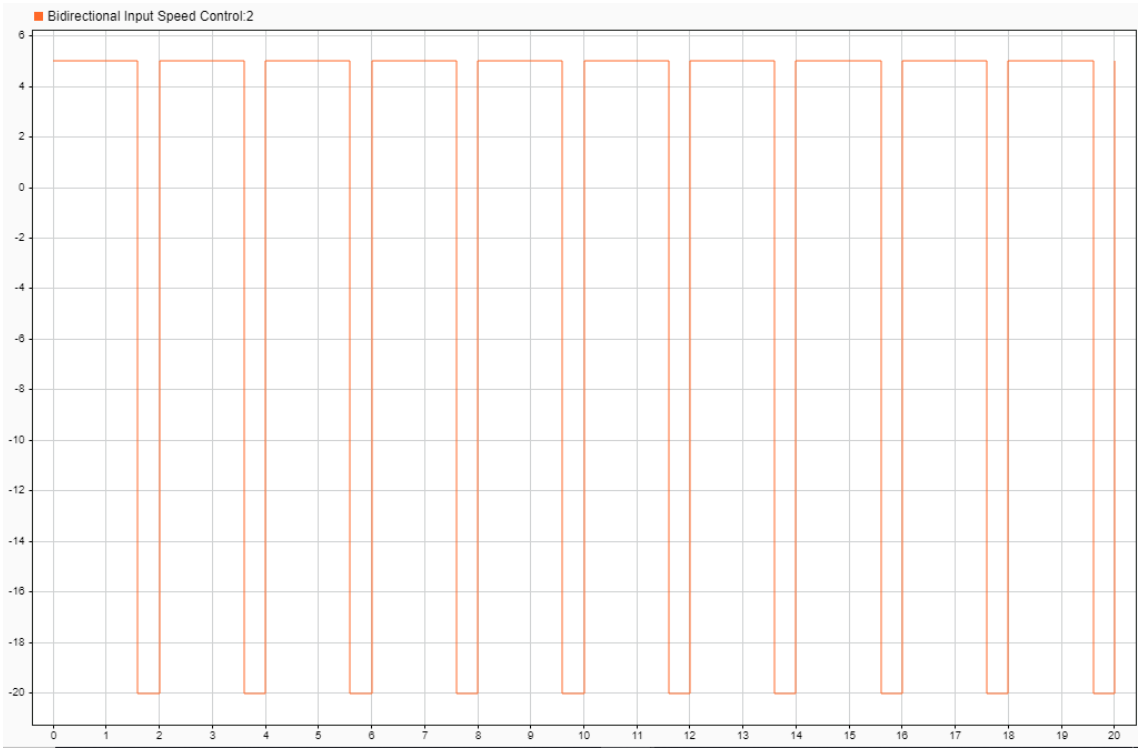

Figure 31 - Bidirectional speed control input for continuous rotation varying speeds

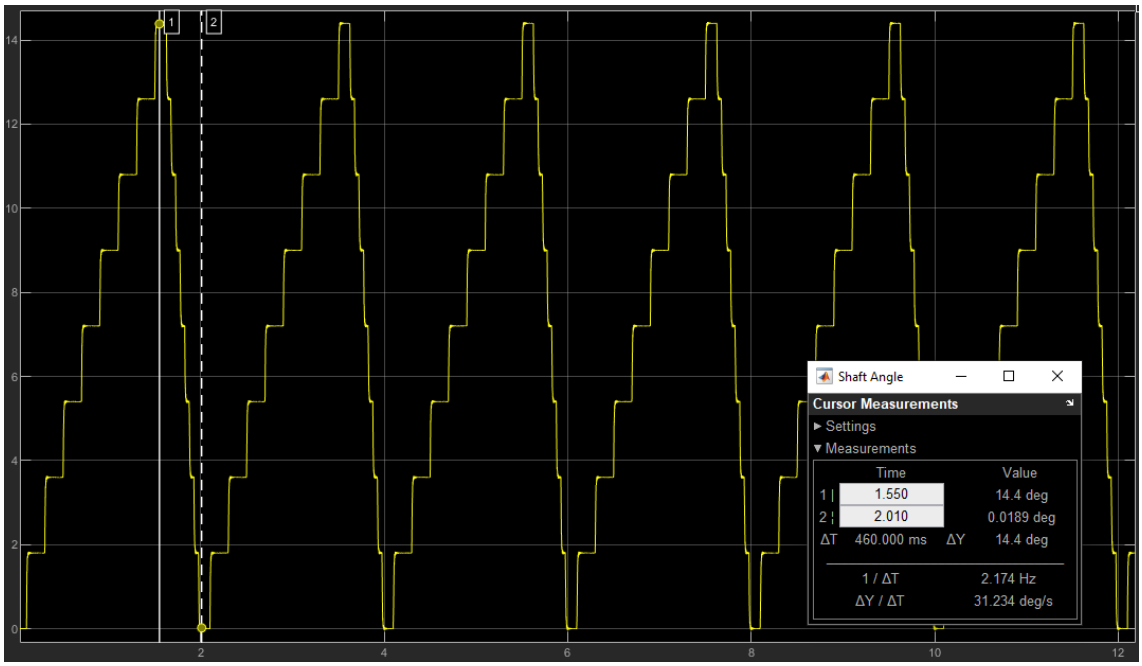

Figure 32 - Bidirectional speed control output for continuous rotation at varying speeds

In this scenario, the motor rotates for 1.6 seconds at five steps per second and then returns to its starting position at 20 steps per second for 0.4 seconds to ensure the same number of steps in both directions. The values selected for the rate of rotation and its corresponding time duration were calculated to prevent discrepancies caused by additional steps taken in one direction or the other, resulting in a skewed motor response.

XX

The third case of bidirectional rotation has the same speed for both directions of motion. It works similarly to the XY case described above, the only difference being that the two speeds are equal. This is the simplest case for motor control, requiring the input signal to switch between two amplitudes and maintain them for a cycle's same duration of time. The input signal and its corresponding motor movement are displayed in Figure 33 and Figure 34, respectively.

Figure 33 - Bidirectional speed control input for same rotational speed

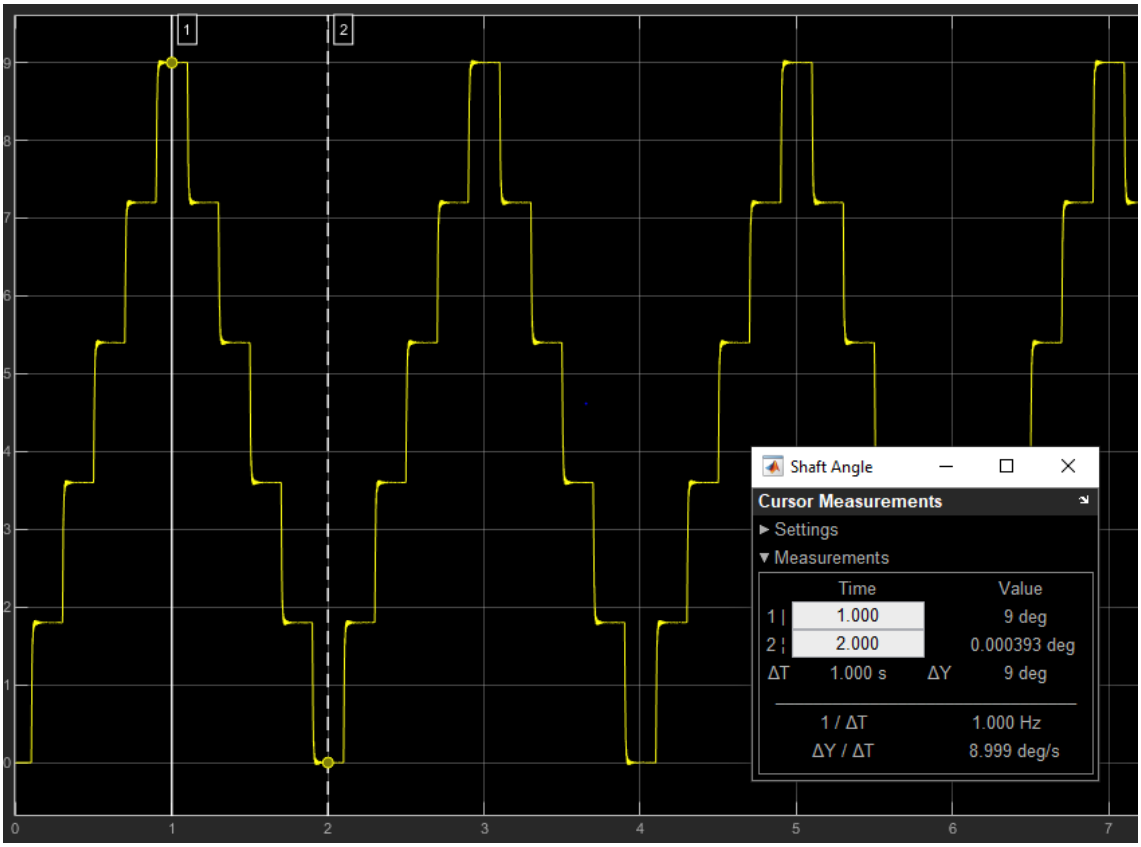

Figure 34 - Bidirectional speed control output for same rotational speed (degrees vs. time)

The graph shows the motor rotating 9 degrees (5 steps) in one direction in a second, thus operating at a frequency of 0.5Hz.

4.8.3 Autodesk's TinkerCad Simulation

Autodesk's TinkerCad platform is popular in maker spaces because it provides various tools and options for creating 3d printed designs and basic simulations for electrical components and circuitry. Its library for electrical circuits contains a limited number of parts and options. However, they are sufficient for creating a proof-of-concept for a motor driver circuit that can control the motor's speed and direction of rotation as its output. The library provides the Arduino Uno R3, which is a microcontroller board based on the ATmega328P microcontroller. It has six output pins for Pulse Width Modulation (PWM) out of a total of 22 pins. PWM is used to control the speed of DC motors. For a stepper motor, any of the digital input/output pins can be utilized to control the activation of its phases. Alternatively, the stepper motor movement can be controlled using a potentiometer connected to an analog input pin. In the simulation, pins 8-11 are assigned for stepper motor control, providing the required signals for the driver IC. The sequence of energizing the motor phases determines the direction of rotation.

There are three techniques available for controlling the rotation of a stepper motor. These are called full-step, half-step, and micro-stepping techniques. The program running on the microcontroller governs the stepping technique. Libraries that contain the coding for stepper motor control are freely available, and the functions can be used to produce the desired speed and position control a stepper motor's rotation. The code is compiled into a hex file format and transferred to the microcontroller memory in a process known as burning the microcontroller. The advantage of using an Arduino board is its built-in USB port which can be connected to a computer to perform the burning process, and without moving the microcontroller, the same board can be connected to the motor control circuitry. This reduces the need for separate burning and microcontroller circuit beds, thus simplifying the entire procedure. Following is the code for controlling a stepper motor that completes one revolution in 200 steps. The program rotates the motor five steps clockwise and then counterclockwise, at the rate of 5 steps in a second in both directions.

```
/*
 Stepper Motor Control - one revolution

 This program drives a unipolar or bipolar stepper motor.
 The motor is attached to digital pins 8 - 11 of the Arduino.

 The motor rotates back and forth with a pause of
half a second between each movement.
 */
```

```
#include <Stepper.h>

const int stepsPerRevolution = 200;  // 1.8 degrees step size

// initialize the stepper library on pins 8 through 11:
Stepper myStepper(stepsPerRevolution, 8, 9, 10, 11);

void setup() {
  // set the press speed at 5/200rpm (5 steps every second):
  myStepper.setSpeed(5/200);
  // initialize the serial port:
  Serial.begin(9600);
}

void loop() {
  // step one revolution  in one direction:
  Serial.println("clockwise");
  myStepper.step(5);
  delay(500);

  // step one revolution in the other direction:
  Serial.println("counterclockwise");
  myStepper.step(-5);
  delay(500);
}
```

The code above makes use of the stepper library built for controlling stepper motors. Using these readily available libraries and their functions makes it easier to modify parameters and control the stepper motor rotation properties to execute different types of excitation modes for their operational characteristics, depending on the fatigue testing or loading requirements. In this case, the code is implementing the XX speed control test scenario where the motor is rotating in both directions at the same speed throughout the operation.

The simulation is driving a bipolar stepper motor which is evident from the four wires corresponding to the end terminals of its two coils. Since it is a bipolar motor, an H-bridge circuit is required to control its speed and direction of rotation. The L293D IC is a popular H–bridge type driver IC utilized for this purpose. It can work with a voltage range of 5V to 36V and handle up to 1.2A of current. The shape and size, resistance to temperature, easy control, and comparatively low price make it a popular driver option for dc motors. The outputs from the microcontroller board are fed into the driver IC at the appropriate input pins. The output from the driver IC is fed into the stepper motor coils resulting in its discrete stepwise rotation.

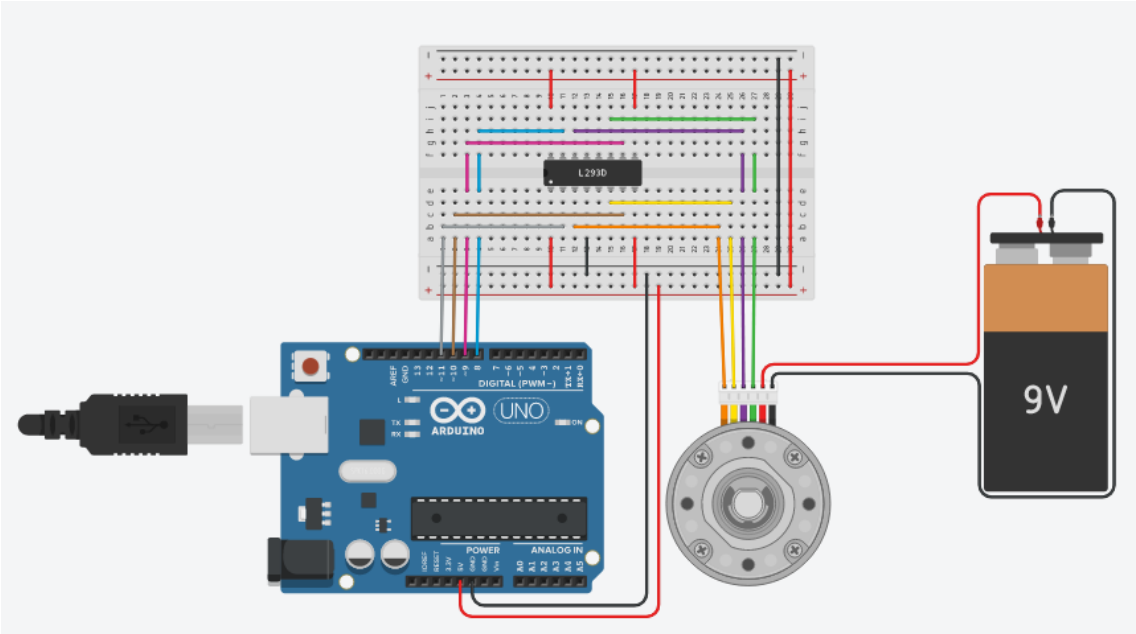

Figure 35 - TinkerCad circuit model for bipolar stepper motor control using Arduino

4.9 Motor Control Circuitry

The essential components of a motor drive circuit include drivers, power supply, and microcontrollers [23]. The drive is a circuit that takes DC or AC voltage and converts it into pulses that rotate the motor shaft. The power supply ensures regulated voltage and allows for the required current draw for the motor application. The controller is the computation unit, which moves the motor as needed by controlling the energizing motor windings sequence. In general motor applications, ready-made integrated circuits can be used, eliminating the complexity of using electrical components, such as resistors, capacitors, transistors, etc., to assemble and design a driver circuit with the same functionality.

A permanent magnet stepper motor usually contains two windings [22]. The driver is responsible for energizing these windings in the correct order to produce the desired motion. A bipolar stepper motor has no center tap in its windings and thus requires the direction of the current to be altered by the driver to switch between motor rotation directions. The rotation is accomplished by applying a particular sequence of forwarding and reverse currents across the two windings. Reversal of the current direction is achieved by using an H-bridge as the driver on each winding. Figure 36 illustrates the h-bridge circuit that would control one motor winding. Two transistors are connected to one PWM input signal. When activated, the two transistors work together to complete the circuit—allowing current flow in one direction. Only one PWM input is active at a time. As discussed earlier, ICs such as the L293D implement the h-bridge functionality for two motor windings, simplifying circuit design and control. However, in

applications that require even higher current flow, the circuit can be designed using discrete transistor or MOSFET components in the same configuration shown in Figure 36. A complete h-bridge circuit driver for a stepper motor is illustrated in Figure 20.

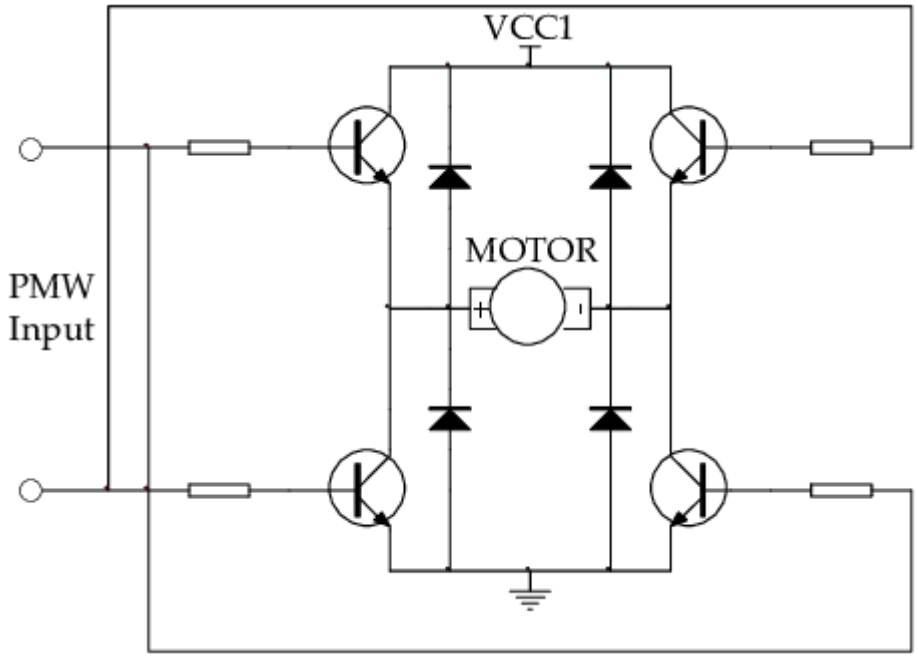

Figure 36 - Schematic drawing of an H-bridge motor driver circuit [28]

The driver circuit allows the current flow to the motor windings as directed by the microcontroller PWM input. Usually, the microcontroller cannot deliver the required current for the motor application since they are a low-powered device. Consequently, a power supply is required for the stepper motor. This is achieved via a voltage-regulated power supply that can maintain the required voltage and provide the current needed to the driver circuit. Figure 37 shows the circuit utilizing a regulator with a TIP2955 transistor to handle currents of up to 5 amperes while keeping the voltage constant. The transistor can require a heat sink for high current applications running for longer durations [23].

Finally, many microcontrollers can serve as computational units for motor control [23]. The Arduino microcontroller board has the advantage of built-in peripherals for expanding system functionality. Furthermore, the board enables easy reprogramming of the controller through a USB connection port. It is possible to achieve this with other microcontrollers, but that would require further effort and time along with the risk of errors. Arduino provides a robust and reliable option at a low cost.

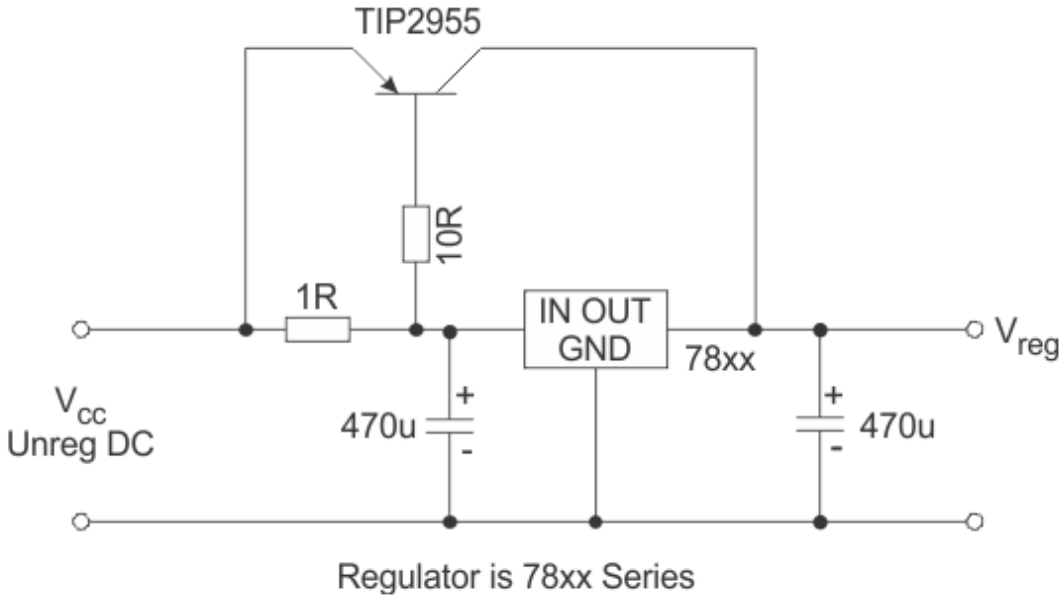

Figure 37 – Voltage-regulated power supply unit [23]

5 RESULTS AND ANALYSIS

The goal of the thesis was to design & implement a solution for a "Low-Cost Fatigue Tester for Makerspaces." The FTM aims to put 3D printed parts under constant amplitude axial load testing, with a low cycle frequency of 0.5 Hz, a torque of up to 70 Nm, and a stroke length of 5mm. This research work explores the phenomenon of fatigue and the importance of testing for it. Previous research on fatigue testing and analyses and the construction of fatigue testing machines provide guidance and instruction to tackle the problem statement. The study identified essential components of an FTM, and the attempts to design a cost-effective solution gave direction to this research work.

A list of steps in the form of a flow chart describes the framework for designing an FTM utilizing electric motors. A selection criterion is detailed to assist in selecting the motor for the application. The hybrid bipolar stepper motor has been identified as the correct choice as it fulfills requirements for high torque, step accuracy, and speed. A motor driver circuit simulation for a bipolar stepper motor, using simulation tools provided by MATLAB/Simulink, is designed to achieve the input control for the motor and produce the required motion. The different motor control patterns executed during simulation demonstrate the system's flexibility for different types of fatigue testing and compatibility with various mechanical systems for transmission of rotation to linear motion. Since the mechanical system will determine the final torque and motion characteristics of the FTM and it is beyond the scope of this research, it is necessary to demonstrate an actuation system capable of adjusting to the requirements.

Furthermore, the simulation utilizes a motor model readily available in the Simulink library, which is a low torque model. The simulation also excludes any mechanical gear system to demonstrate linear movement and torque conversion. These gaps in the current simulation allow future work by utilizing high torque motor characteristics and mechanical model simulations to build on the present work.

The implementation of the motor actuation system has been briefly discussed along with component suggestions to handle high power applications if required. Due to time constraints, the physical implementation of the proposed FTM could not be achieved. Future work on this thesis could be continued by implementing the simulated system on a PCB with a circuit simulation software such as Proteus using the recommended

circuit components and performing practical testing with a mechanical system converting the rotation of the stepper motor to linear motion according to the required configuration, integrating force sensors, interfacing a cycle counter, and finally generating an S-N curve by subjecting the auxetic cell to a constant amplitude, uniaxial, high cycle fatigue test. Moreover, the motor selection criteria and the FTM design framework suggested in this thesis can be improved upon based on any gaps identified during its application and fatigue test results.

6 CONCLUSION

The design of the FTM required an electrical actuator and considering the needed 70Nm torque and frequency of 0.5Hz in this application, as well as the impact of cost, a hybrid bipolar stepper motor was selected as the suitable choice. The motor control design is simulated in MATLAB/Simulink using a step block for input, a control block to provide PWM and direction modulation for the motor, a driver block to energize the phases to maintain required rotation direction, the bipolar stepper motor, and a scope at the output of the motor to measure shaft angle.

As the scope of this thesis does not include the mechanical coupling design of the final FTM, the simulation was used to show the flexibility of the design to accommodate a range of torque and motion characteristics.

When the input to the motor is position controlled, the input signal is given to be a square wave of amplitude 5 and frequency 0.5Hz. This drives the motor 5 steps in clockwise direction and upon the change of the amplitude in the input wave, the motor rotates 5 steps in the anti clockwise direction at the same frequency as the input. Correcting for the offset of the motor rotation, and the step angle of 1.8 degrees of the motor, the angle of rotation during each cycle is seen to be 9 degrees in each direction. This results in the required compression and decompression motion needed to be achieved in this application. This mode has constant speed in each direction, for variable speeds in different directions, speed control mode has to be simulated.

Speed control is achieved by manipulating the input signal to the control block. The speed control is simulated in both unidirectional and also back and forth rotation. In unidirectional rotation, when a step signal input of amplitude 10 was provided for 10 seconds, the shaft position constantly increased from 0 to 180 degrees, at a rate of 10 steps/sec each step being 1.8 degrees, after which the position remained constant, indicating the motor did not rotate further when input went to 0. By modifying the input signal to jump to different amplitudes, different motor speeds can be achieved at different intervals as required. This is seen when the signal jumps from amplitude 10 to 15 at 10 second mark, causing the motor to rotate to 180 degrees followed by an additional 270 degrees in the next 10 seconds. This shows the required variation in

speed and frequency that can be achieved if a cam based mechanical coupler is selected in the next stage of design.

In bidirectional speed control simulation, three scenarios are simulated. The X0Y simulation has clockwise rotation, followed by a pause, followed by an anticlockwise rotation with varying speeds of motion in each direction. The input is at 5 for 1 sec, followed by 0 for 0.5 sec and -10 for another 0.5 sec. The result for this input is a 9 degree rotation in clockwise direction in 1 second, holding at that position for 0.5 sec and 9 degree rotation in the opposite direction in 0.5 seconds, simulating the scenario where in the decompression speed is half the compression speed, and the cell is held at complete closure for one quarter of the fatigue cycle.

In the XY scenario, the motor is required to rotate clockwise and anticlockwise without any pause. The step input signal amplitude of 5 determines the speed of the clockwise rotation, and the time of the input being 1.6 sec determines the time of the rotation, resulting in 1.6 seconds of rotation at 5 steps per rotation. The input drops to -20 at 1.6 sec and stays there for 0.4 sec, causing the motor to turn at 20 steps per second for 0.4 seconds and return to its initial position. This simulation is useful for applications when the compression speed has to be slower than the decompression speed and the cell does not have to be held at complete close position.

The XX scenario is also simulated where the speed of rotation in both directions is the same and there is no pause between the rotations. The input signal has a constant amplitude in either direction, and is held there for the same time duration resulting in the motor position to also have a 50% cycle duration. The input is given an amplitude of 5 and the motor rotates 9 degrees in each direction in 5 steps in one second, resulting again in the required 0.5 Hz frequency.

It is established that following the matrix for the motor selection and utilizing the bidirectional rotation which is position or speed controlled, this setup is capable of delivering the required 0.5 Hz frequency. Also it can provide a range of frequency controls in both directions by simply manipulating the input signal. The mechanical coupling attached to the motor would determine the final torque and speed of rotation necessary to achieve it. This gives the mechanical design some leverage to make the needed coupling solutions to implement the design to achieve the torque range of up to 70 Nm.

Futur work could entail modeling of this design first on a breadboard and once the design is seen to be successful to implement the same using a PCB. This would result in having the electric and computational design of the FTM in place. It would then

require the mechanical design including a cam shaft or gear based design to realize the lateral movement for compressing the auxetic cells.

A good addition to the system would be the control options for frequency and needed torque for the fatigue testing from a predefined matrix. As the system is capable of servicing a range of loads, this will increase the usability of the FTM to various applications. Once this is achieved, the overall design would need to be checked for ease of usability and safety of operation, for example in case of failure the system should not cause any harm to the user or material being tested. This will result in a standardized low cost FTM for research and academic purposes.

REFERENCES

[1] Netzev M, Angleraud A, Pieters R. Soft Robotic Gripper with Compliant Cell Stacks for Industrial Part Handling. IEEE robotics and automation letters. 2020;5(4):6821–8.

[2] Gbasouzor AI, Okeke CO, Chima LO. Design and Characterization Of A Fatigue Testing Machine, Proceedings of The World Congress on Engineering And Computer Science 2013 Vol I,2013.

[3] Azeez AA. Fatigue failure and testing methods [bachelor's thesis]. Riihimäki: HAMK University of Applied Sciences; 2013. 32 p.

[4] Banavasi S, Naik P. A Review on Design and Fabrication of Fatigue Testing Machine. International Journal of Novel Research and Development. 2018; 3(5): 5-14.

[5] Quadir A, Chaturvedi SK. Design and development of fully reversed axial loading fatigue testing machine. *International Journal of Advances in Engineering & Scientific Research.*2014; 1(3): 8-17.

[6] Henseler, J. Designing a Control for a Material Fatigue Testing Machine [semester final paper on the Internet]. Munich: GRIN Verlag: 2001 [cited 2021 Mar]. Available from: https://www.grin.com/document/6661

[7] Jurecki R, Pokropiński E, Więckowski D, Żołądek Ł. Design of a Test Rig for the Examination of Mechanical Properties of Rolling Bearings. Management Systems in Production Engineering. 2017;25(1): 22-28. https://doi.org/10.1515/mspe-2017-0003

[8] Lee YL, Pan J, Hathaway R, Barkey M. Fatigue Testing and Analysis: Theory and Practice. Oxford: Elsevier Science & Technology; 2004.

[9] Będkowski W. Assessment of the fatigue life of machine components under service loading - A review of selected problems. Journal of Theoretical and Applied Mechanics. 2014;52(2):443–58.

[10] Santecchia E, Hamouda AMS, Musharavati F, Zalnezhad E, Cabibbo M, El Mehtedi M, et al. A Review on Fatigue Life Prediction Methods for Metals. Advances in materials science and engineering. 2016:1–26.

[11] Pook L. Standard fatigue tests for components. In: European Structural Integrity Society. 1997:203–14.

[12] Fatemi A, Yang L. Cumulative fatigue damage and life prediction theories: a survey of the state of the art for homogeneous materials. International journal of fatigue. 1998;20(1):9–34.

[13] Zenner H, Hinkelmann K. August Wöhler – founder of fatigue strength research: On the 200th anniversary of August Wöhler's birth. Steel construction: design and research. 2019;12(2):156–62.

[14] What is Fatigue Life – S-N Curve - Woehler Curve - Definition | Material Properties [Internet]. Material Properties. 2021 [cited 13 May 2021]. Available from: https://material-properties.org/what-is-fatigue-life-s-n-curve-woehler-curve-definition/

[15] Pugi L, Rindi A, Allotta B, Gori G. Design of an Actuation System for a Fatigue Test RIG. In: Proceedings of EUCOMES 08. Dordrecht: Springer Netherlands; 2009. p. 201–8.

[16] Hoeppner DW. Industrial Significance of Fatigue Problems. In: Fatigue and Fracture [Internet]. ASM International; 1996 [cited 2021 May 29]. p. 0. Available from: https://doi.org/10.31399/asm.hb.v19.a0002348

[17] Fatigue Testing Machine Market Overview, Segments, Competitor Strategies, Industry Outlook, Analysis & Forecast 2018-2028 [Internet]. Future Market Insight. [cited 2021 May 14]. Available from: https://www.futuremarketinsights.com/reports/fatigue-testing-machine-market

[18] Liu Y, Kang G, Gao Q. Stress-based fatigue failure models for uniaxial ratchetting–fatigue interaction. International journal of fatigue. 2008;30(6):1065–73.

[19] Burris M. Stepper Motors vs. Servo Motors: Which Is Best for Your Application? [Internet]. Lifewire. 2021 [cited Jul 7 2021]. Available from: https://www.lifewire.com/stepper-motor-vs-servo-motors-selecting-a-motor-818841#driving-mechanism-steppers-are-more-precise

[20] What is a Servo Motor? - Definition from Techopedia [Internet]. Techopedia.com. 2021 [cited Jul 7 2021]. Available from: https://www.techopedia.com/definition/13274/servo-motor

[21] Maleki, Erfan & reza kashyzadeh, Kazem. (2017). Effects of the hardened nickel coating on the fatigue behavior of CK45 steel: Experimental, finite element method, and artificial neural network modeling. Iranian Journal of Materials Science and Engineering. 14. 81-99. 10.22068/ijmse.14.4.81.

[22] Keim R. How to Choose the Right Driver IC for Stepper Motors [Internet]. All About Circuits. 2018 [cited 2021 Jul 2]. Available from: https://www.allaboutcircuits.com/technical-articles/how-to-select-the-right-driver-ic-for-stepper-motors/

[23] Stepper Motor Driver (Circuit Diagram & Schematic) [Internet]. Electrical 4 U. 2021 [cited 2021 Jul 7]. Available from: https://www.electrical4u.com/stepper-motor-drive/

[24] Condit R, Jones DW. Stepping Motor Fundamentals [Internet]. Microchip Technology Inc.; Available from: http://ww1.microchip.com/downloads/en/AppNotes/00907a.pdf

[25] Shakoor MM. Fatigue life investigation for cams with translating roller-follower and translating flat-face follower systems [Internet]. Iowa State University; 2006. Available from: https://lib.dr.iastate.edu/cgi/viewcontent.cgi?article=2302&context=rtd

[26] Morar A. The Modelling and Simulation of Bipolar Hybrid Stepping Motor by Matlab/Simulink. Procedia Technology. 19(2015):576–83.

[27] All You Need to Know About L293D [Internet]. Maker Pro. 2018 [cited 2021 Jul 7]. Available from: https://maker.pro/custom/projects/all-you-need-to-know-about-l293d

[28] Wu L, Lian Z, Yang G, Ceccarelli M. Water Dancer II-A: A Non-Tethered Telecontrollable Water Strider Robot. International Journal of Advanced Robotic Systems [Internet]. 2011/9//01;8(4). Available from: https://www.researchgate.net/publication/221915427_Water_Dancer_II-A_A_Non-Tethered_Telecontrollable_Water_Strider_Robot